Received: 6 December 2022 | Revised: 25 July 2023 | Accepted: 22 August 2023

DOI: 10.1111/bph.16235

RESEARCH ARTICLE

Pharmacological characterization of SAGE-718, a novel positive allosteric modulator of N-methyl-D-aspartate receptors

Jacob T. Beckley | Teresa K. Aman | Michael A. Ackley | Tatiana M. Kazdoba | Michael C. Lewis | Anne C. Smith | Brandon J. Farley | Jing Dai | Wayne Deats | Ethan Hoffmann | Albert J. Robichaud | James J. Doherty | Michael C. Quirk

Sage Therapeutics Inc, Cambridge, Massachusetts, USA

Correspondence
Jacob T. Beckley, Sage Therapeutics Inc, 215 First Street, Cambridge, MA 02142, USA.
Email: jacob.beckley@sagerx.com

Present address
Michael A. Ackley, Onsero Therapeutics, Boston, MA.

Funding information
Sage Therapeutics

Background and Purpose: Select neuroactive steroids tune neural activity by modulating excitatory and inhibitory neurotransmission, including the endogenous cholesterol metabolite 24(S)-hydroxycholesterol (24(S)-HC), which is an N-methyl-D-aspartate (NMDA) receptor positive allosteric modulator (PAM). NMDA receptor PAMs are potentially an effective pharmacotherapeutic strategy to treat conditions associated with NMDA receptor hypofunction.

Experimental Approach: Using in vitro and in vivo electrophysiological recording experiments and behavioural approaches, we evaluated the effect of SAGE-718, a novel neuroactive steroid NMDA receptor PAM currently in clinical development for the treatment of cognitive impairment, on NMDA receptor function and endpoints that are altered by NMDA receptor hypoactivity and assessed its safety profile.

Key Results: SAGE-718 potentiated GluN1/GluN2A-D NMDA receptors with equipotency and increased NMDA receptor excitatory postsynaptic potential (EPSP) amplitude without affecting decay kinetics in striatal medium spiny neurons. SAGE-718 increased the rate of unblock of the NMDA receptor open channel blocker ketamine on GluN1/GluN2A in vitro and accelerated the rate of return on the ketamine-evoked increase in gamma frequency band power, as measured with electroencephalogram (EEG), suggesting that PAM activity is driven by increased channel open probability. SAGE-718 ameliorated deficits due to NMDA receptor hypofunction, including social deficits induced by subchronic administration of phencyclidine, and behavioural and electrophysiological deficits from cholesterol and 24(S)-HC depletion caused by 7-dehydrocholesterol reductase inhibition. Finally, SAGE-718 did not

Abbreviations: 24(S)-HC, 24(S)-hydroxycholesterol; EC_{50}, half maximal effective concentration; EcoG, electrocorticogram; EEG, electroencephalogram; E_{max}, maximal efficacy; EPSP, excitatory postsynaptic potential; MEA, multi-electrode array; NRE, anti-NMDA receptor encephalitis; PAM, positive allosteric modulator; PCP, phencyclidine; PK, pharmacokinetics; PPC, planar patch clamp; PTSD, post-traumatic stress disorder; PTZ, pentylenetetrazole; TEVC, two-electrode voltage clamp; SI, social interaction; SLOS, Smith–Lemli–Opitz syndrome.

produce epileptiform activity in a seizure model or neurodegeneration following chronic dosing.

Conclusions and Implications: These findings provide strong evidence that SAGE-718 is a neuroactive steroid NMDA receptor PAM with a mechanism that is well suited as a treatment for conditions associated with NMDA receptor hypofunction.

KEYWORDS

cognitive dysfunction; neuroactive steroids; neuropharmacology, pharmacodynamics, allosteric modulation; N-methyl-D-aspartate receptor; translational pharmacology

1 | INTRODUCTION

N-methyl-D-aspartate (NMDA) receptors are **ionotropic glutamate receptors** expressed throughout the CNS and are critical for excitatory synaptic signalling and synaptic plasticity (Traynelis et al., 2010). Structurally, all known NMDA receptors are heterotetramers, consisting of two obligatory **GluN1** subunits and two GluN2 (**A**, **B**, **C**, **D**) or GluN3 (**A**, **B**) subunits (Lü et al., 2017). NMDA receptors containing different GluN2 and GluN3 subunits have distinct gating, permeation and agonist affinities and are expressed differentially between cell types and brain regions. GluN2-containing NMDA receptors are unique among the synaptic receptors, requiring binding of two ligands, **glycine** and **glutamate**, in combination with the relief of voltage-dependent magnesium (Mg^{2+}) block to open an ion conductive pore that allows the influx of Na^{+} and Ca^{2+} ions. Flow of Ca^{2+} through NMDA receptors is particularly important for neuronal function because Ca^{2+} ions activate signalling cascades that lead to synaptic strengthening, which is crucial for learning and memory (Nicoll & Roche, 2013). Conversely, impaired NMDA receptor function can lead to altered synaptic transmission, modified synaptic plasticity, and increased glutamate excitotoxicity or cell death (Q. Zhou & Sheng, 2013).

Given the important role of NMDA receptors in neuronal signalling, their dysfunction is linked to a range of neurological and psychiatric conditions, including schizophrenia, sudden-onset psychosis, post-traumatic stress disorder (PTSD) and depression, and neurodegenerative diseases, such as Huntington's disease, Parkinson's disease, Alzheimer's disease and several types of dementia (Anticevic et al., 2012; Fernandes & Raymond, 2009). Potentiating the activity of NMDA receptors is a promising therapeutic strategy for conditions that are caused by their hypofunction, such as schizophrenia, encephalopathies (e.g., anti-NMDA receptor encephalitis [NRE]) and forms of dementia (Geoffroy et al., 2022). Positive modulators of NMDA receptors have shown beneficial effects in preclinical models of Alzheimer's disease, Dravet syndrome (Hanson et al., 2020) and PTSD (B. Lee et al., 2022). However, demonstration of efficacy with novel treatments for cognitive impairment or other conditions associated with NMDA receptor hypofunction in patient populations is needed.

Some neuroactive steroids derived from cholesterol or the concomitant biomimetic pathway tune the function of both excitatory and inhibitory neurotransmission through allosteric modulation of membrane-bound proteins (Paul et al., 2013). The primary metabolite of cholesterol in brain is the oxysterol **24(S)-hydroxycholesterol** (24(S)-HC), which is a potent positive allosteric modulator (PAM) of NMDA receptors (Ishikawa et al., 2018; Paul et al., 2013). 24(S)-HC plays an important role in maintaining neuronal activity (Sun et al., 2016), and mice lacking **CYP46A1**, the enzyme that produces 24(S)-HC, have significantly reduced 24(S)-HC levels and substantial behavioural learning and memory deficits (Kotti et al., 2006). Impaired synthesis and trafficking of neuroactive steroids have been implicated in neurodegenerative disorders and other neurological conditions (Gamba et al., 2021; Leoni et al., 2002, 2008). Specifically, reduced levels of 24(S)-HC have been demonstrated in Huntington's disease (Leoni et al., 2013) and in more severe cases of Alzheimer's disease (Papassotiropoulos et al., 2000).

We recently disclosed **SAGE-718**, which acts as a PAM of NMDA receptors with drug-like properties (Hill et al., 2022; Figure 1a). Here, we

What is already known

- N-methyl-D-aspartate (NMDA) receptor hypofunction may be associated with cognitive impairment.
- SAGE-718 is a novel, investigational oral NMDAR receptor positive allosteric modulator.

What does this study add

- SAGE-718 increases NMDA receptor activity across electrophysiological platforms and rescues deficits in preclinical NMDA receptor hypofunction models.
- SAGE-718 did not produce epileptiform activity or neurodegeneration in non-clinical models.

What is the clinical significance

- SAGE-718 is being evaluated for the treatment of cognitive impairment associated with neurodegenerative disorders.

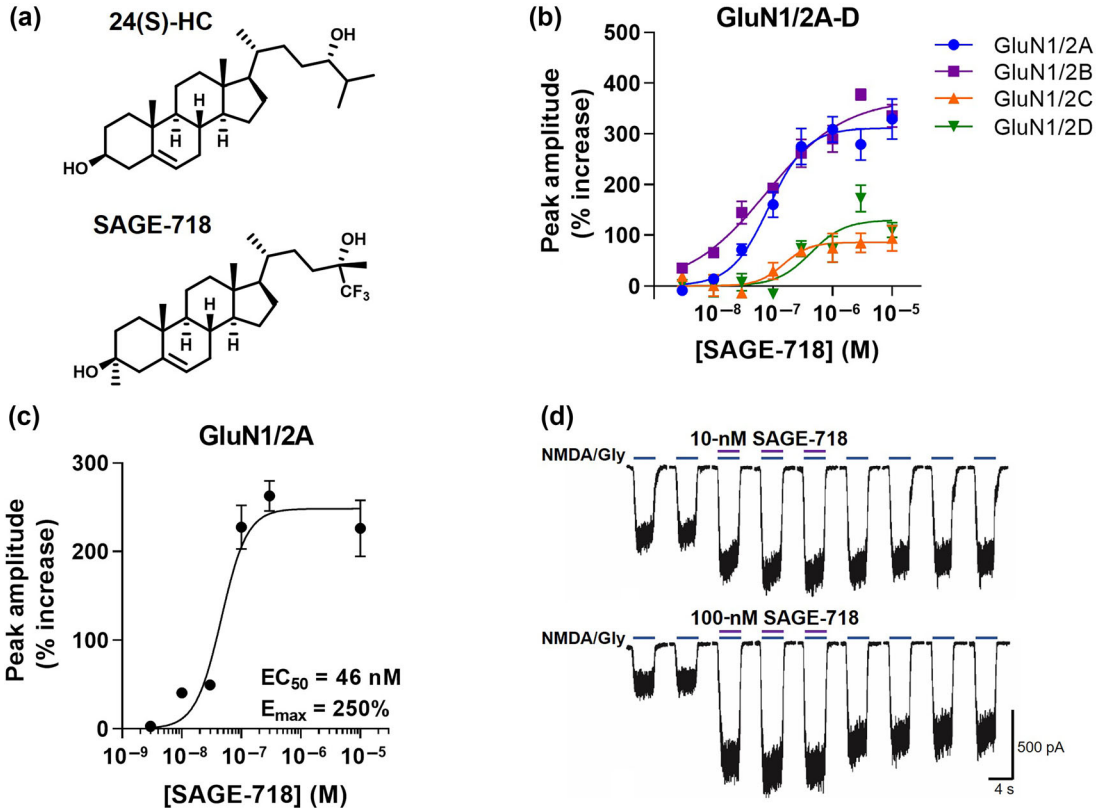

FIGURE 1 SAGE-718 is a pan-NMDA receptor positive allosteric modulator (PAM). (a) 24(S)-hydroxycholesterol (24(S)-HC) (top) and SAGE-718 (bottom) structure. (b) Concentration–response of SAGE-718 potentiation of GluN1/GluN2A–D receptor-mediated currents recorded on the IonWorks Barracuda automated patch-clamp platform with HEK cells stably expressing NMDA receptors. NMDA receptor currents were evoked with submaximal 0.8 μM of glutamate and saturating 50 μM of glycine. Potency (EC_{50} in nM) and efficacy (E_{max} in percentage increase over vehicle) values are reported in Hill et al. (2022) and are (with 95% confidence interval) GluN1/2A: EC_{50} = 86 (56–130), E_{max} = 310 (280–350), Hill slope (h) = 1.4; GluN1/2B: EC_{50} = 79 (42–150), E_{max} = 370 (320–410), h = 0.7; GluN1/2C: EC_{50} = 150 (63–350), E_{max} = 86 (62–110), h = 2 (constrained); GluN1/2D: EC_{50} = 430 (170–1100), E_{max} = 130 (90–170), h = 1.5 (n = 1–3 plates per subtype; 4 wells per concentration per plate). (c) Concentration–response curve of SAGE-718 potentiation of NMDA receptor-mediated currents recorded under voltage clamp on HEK cells stably expressing GluN1/2A (n = 3–5 cells per concentration); EC_{50} = 46 (32–67), E_{max} = 250 (210–280), h = 2 (constrained). (d) Representative NMDA receptor traces evoked by submaximal 30 μM of NMDA and 5 μM of glycine (blue line; sub-saturating) in HEK cells, with the addition of 10 (top) or 100 nM (bottom) of SAGE-718 for three evoked currents following two baseline applications without SAGE-718.

show that SAGE-718, with a mechanism in line with other neuroactive steroid NMDA receptor PAMs and the endogenous PAM, 24(S)-HC (Emnett et al., 2015; Paul et al., 2013; Tang et al., 2023), reverses behavioural and in vivo electrophysiological impairments produced by acute or persistent hypofunction of NMDA receptors, while maintaining a wide safety margin. The data described here support SAGE-718 as an efficacious neuroactive steroid NMDA receptor PAM that is well suited to treat conditions associated with NMDA receptor hypofunction.

2 | METHODS

2.1 | In vitro pharmacology

2.1.1 | Automated patch-clamp electrophysiology

IonWorks Barracuda (IWB) automated electrophysiology platform (Molecular Devices, San Jose, CA, USA) was used as previously described (Althaus et al., 2020; La et al., 2019). Modulation of NMDA receptors was assessed using electrophysiological recordings of human embryonic kidney cells (HEK293) stably expressing recombinant GluN1/2A (Charles River Cat# CT6120; GenBank acc. nums NM_007327.2 and NM_000833.2), GluN1/2B (Charles River Cat# CTN6121; NM_007327.2 and NM_000834.3), GluN1/2C (Charles River Cat# CT6133; NM_007327.2 and NM_000835.3) or GluN1/2D (Charles River Cat# CT6134; NM_007327.2 and NM_000836.2) receptors. Cell line validation information is available on file (Charles River Laboratories, Cleveland, OH, USA). Whole-cell patch-clamp recordings (−70 mV) were conducted at room temperature using an intracellular solution containing (in mM) 50 CsCl, 90 CsF, 2 $MgCl_2$, 5 EGTA and 10 HEPES, pH 7.2 (CsOH). Extracellular solution contained (in mM) 137 NaCl, 1 KCl, 5 $CaCl_2$, 10 HEPES and 10 glucose, pH 7.4 (NaOH). Test articles were serially diluted from a stock solution to test concentrations of 3–10,000 nM, half-log increments with final concentrations of 0.3%–0.6% DMSO and 0.01% Kolliphor EL. Planar patch clamp (PPC) wells were loaded with 11 μl of

extracellular solution and 9 μl of cell suspension. The holding potential was stepped to −40 mV during application of the test compounds and/or co-agonists, and currents (0.8 μM of glutamate [EC_{20}] and 30 μM of glycine [saturating]) were measured before and after a 5-min preincubation with 2× concentrated test article. Data acquisition and analysis was performed using the IonWorks software (Molecular Devices Corporation, Union City, CA, USA). The effect of each concentration (n = 4 per plate) of the test article was calculated as a percentage increase in peak amplitude over the mean NMDA receptor peak current from wells exposed to vehicle within the same plate. For subtypes that were tested across multiple plates, the means and variances of each test concentration were pooled.

The 24(S)-HC interaction assay was conducted using the SyncroPatch 384i automated patch-clamp platform (Nanion, Munich, Germany) with a HEK cell line expressing recombinant human GluN1/GluN2A (GenBank acc. nums NP_015566.1 [GluN1] and NP_001127880 [GluN2A]; RRID: CVCL_C9E4) under the control of a tetracycline-inducible expression system. Cell line validation information is available on file (SB Drug Discovery, Glasgow, UK). Extracellular solution contained (in mM) 140 NaCl, 4 KCl, 5 $CaCl_2$, 10 HEPES and 5 glucose, pH 7.4 (NaOH), and 0.2% DMSO and 0.01% Kolliphor EL. Internal solution contained (in mM) 120 CsF, 10 EGTA, 10 NaCl, 10 HEPES, 4 NaATP and 2 $MgCl_2$, pH 7.2 (CsOH). Automated whole-cell patch-clamp recordings (−80 mV) were performed using multi-hole high-resistance chips (2–3 MΩ). Currents were leak corrected and sampled at 5 kHz. A fast application protocol was used to elicit currents with 1 μM of glutamate (sub-saturating)/100 μM of glycine (saturating) twice to demonstrate reproducibility of the NMDA receptor current. Next, 24(S)-HC (0, 0.001, 0.01, 0.1 or 1 μM) was added to the well for 60 s preincubation, and then currents were measured again with co-agonists. SAGE-718 was then added at 1 nM to 3 μM, half-log increments; there were three to eight wells per concentration and NMDA receptor currents were assayed again in the presence of both 24(S)-HC and SAGE-718. After a washout period, a saturating concentration of agonist (100 μM of glutamate/100 μM of glycine) was applied. The voltage protocol generation data collection and analysis were performed on PatchControl 384/DataControl 384 Version 1.9 (Nanion). The change in peak amplitude was determined using the following equation:

$$\textit{Change in Peak Amplitude} = ((I_{comp}/I_{control}) - 1) * 100$$

where $I_{control}$ is the NMDA receptor current amplitude in the presence of 24(S)-HC only and I_{comp} is the current amplitude in the presence of both 24(S)-HC and the test compound.

2.1.2 | Manual patch-clamp electrophysiology

Whole-cell recordings

HEK293 cells stably transfected with NMDA GluN1/GluN2A receptors (GenBank acc. nums NP_015566.1 [GluN1] and NP_000824.1 [GluN2A]; RRID: CVCL_C9D2), Ltk cells stably transfected with cDNA for recombinant $GABA_A$ α1β2γ2 receptors (GenBank acc. nums NP_000797.2 [α1], NP_000804.1 [β2] and NP_000807.2 [γ2]; RRID: CVCL_C9E7) and Chinese hamster ovary (CHO) cells transiently transfected with cDNA for recombinant $GABA_A$ α4β3δ receptors (GenBank acc. nums NP_000800.2 [α4], NP_000805.1 [β3] and NP_000806.2 [δ]) were used to investigate the modulatory effects of SAGE-718 on NMDA and **$GABA_A$ receptors**. Cell line validation information is available on file (B'SYS GmbH, Witterswil, Switzerland). Cell culture dishes were placed on the dish holder under a microscope, and the bath solutions were continuously perfused at 1 ml·min^{-1}. Studies were conducted at room temperature. Electrophysiological recordings were performed using an extracellular solution containing (in mM) 137 NaCl, 4 KCl, 1.8 $CaCl_2$, 1 $MgCl_2$, 10 HEPES and 10 D-glucose, pH 7.4 (NaOH). Intracellular solution contained (in mM) 130 KCl, 1 $MgCl_2$, 5 Mg-ATP, 10 HEPES and 5 EGTA, pH 7.2 (KOH). Compounds were made into a 10-mM stock solution in DMSO with 0.02% Kolliphor EL. A gigaohm seal was formed with a glass pipette (2.5–6.0 MΩ of resistance), and cells were held at −80 mV. For recordings from NMDA receptors, once a stable seal was established, a Mg^{2+}-free extracellular solution was perfused into the chamber. Signal acquisition was performed using an EPC-10 amplifier (HEKA Electronics) with PatchMaster software (HEKA Electronics). NMDA receptor current was evoked twice with sub-saturating agonists of 30 μM of NMDA and 5 μM of glycine so that baseline activity could be established, and then a single concentration of SAGE-718 (0.003, 0.01, 0.03, 0.1, 0.3 or 10 μM; one concentration per cell; at least n = 3 per concentration) was washed onto the cell for 30 s and then the NMDA receptor current was evoked in the presence of SAGE-718. For $GABA_A$ receptor recordings, each concentration of SAGE-718 (0.01, 0.1, 1 and 10 μM) was analysed in n = 3 isolated cells of each $GABA_A$ receptor subtype. $GABA_A$ receptor inward currents were measured upon application of submaximal GABA concentration (2 μM) to patch-clamped cells. Both $GABA_A$ receptor subtypes were stimulated by two applications of 2 μM of **GABA**, followed by increasing concentrations of SAGE-718 and 2 μM of GABA. Recordings were analysed by comparing the current amplitudes with those from control conditions (only NMDA/Gly or only GABA) measured in the pre-treatment phase of the same cell. The amount of current block/stimulation was calculated as percentage of control. Data from at least three individual experiments for NMDA receptors and six experiments for $GABA_A$ receptors per test item and application method were collected, and the corresponding mean values and standard deviations were calculated.

For electrophysiology experiments with **ketamine**, a 10-mM stock of ketamine hydrochloride was diluted in Mg-free bath solution with and without agonists and 10 μM of SAGE-718. Receptors were activated with ∼EC_{90} of the partial agonist NMDA (300 μM) and the saturating agonist glycine (100 μM), which is expected to activate receptors ∼70% compared with the full agonist glutamate (Hedegaard et al., 2012). These agonist conditions were selected to maximize current size to accurately measure ketamine blocking rates while also leaving room for receptor modulation by SAGE-718. To maintain cell viability during extended agonist applications, the effects of SAGE-718 on ketamine block were compared with those of vehicle by

preincubation in separate cells with either 10 μM of SAGE-718 (n = 5) or vehicle (n = 6) for 30 s and SAGE-718 or vehicle was included in all recording solutions. NMDA receptors were activated with agonists for 10 s, and 0.6 μM of ketamine (IC_{50} = 0.59 μM) was applied for 10 s before a 20-s washout in the presence of agonists. The time courses of the current decrease upon application of ketamine and increase with ketamine washout were fit with a mono-exponential time course. The onset (block rate) and offset (unblock rate) were calculated, and channel block kinetics were compared with and without SAGE-718. Data from at least five individual experiments per experiment type were collected, and the corresponding mean values and standard error of the mean (SEM) were calculated.

Two-electrode voltage clamp

The effect of SAGE-718 on different NMDA receptor subtypes (GluN1/GluN2A, 2B, 2C and 2D), as well as the response of SAGE-718 to NMDA receptor co-agonists (glutamate, glycine and **D-serine**), was evaluated on human NMDA receptors transiently expressed in *Xenopus* oocytes. *Xenopus laevis* stage VI oocytes (Xenopus one Inc, Dexter, MI, USA) were digested with Collagenase Type 4 (Worthington-Biochem, Lakewood, NJ, USA) solution (850 μg·ml^{-1}, 15 ml for a half ovary) in Ca^{2+}-free Barth's solution that contained (in mM) 88 NaCl, 2.4 $NaHCO_3$, 1 KCl, 0.33 $Ca(NO_3)_2$, 0.41 $CaCl_2$, 0.82 $MgSO_4$ and 10 HEPES (pH 7.4 with NaOH) supplemented with 100 μg·ml^{-1} of gentamycin and 40 μg·ml^{-1} of streptomycin. Oocytes were maintained in normal Barth's solution at 15°C. For experiments with human and mouse receptors, injection of cDNA encoding human GluN1/2A-2D was performed at a ratio of 1:1 as previously described (Hogg et al., 2008), and mRNA encoding GluN1 and GluN2A was injected for dog and rat receptors.

Recordings were performed at 18°C and cells were perfused with OR2 medium containing (in mM) 88 NaCl, 2.5 KCl, 5 HEPES and 2.5 $BaCl_2$, pH 8. All solutions contained 0.2% Kolliphor EL to improve SAGE-718 solubility and delivery. Currents evoked by glutamate or other agonists were recorded by an automated process equipped with standard two-electrode voltage-clamp (TEVC) configuration (−80 mV) and a GeneClamp amplifier (Axon Instrument, Foster City, CA, USA). NMDA receptor currents were first evoked with a test pulse of 100 μM of glutamate and 10 μM of glycine for 30 s. Cells displaying a robust current were used for subsequent measurements. For NMDA receptor subtype recordings, after recording the cells in control condition for 2 min, subsequent currents were evoked with subsaturating concentration of glutamate (GluN2A: 0.3 μM; GluN2B: 2 μM; GluN2C: 0.5 μM; GluN2D: 3 μM) and saturating glycine (10 μM) and escalating concentrations of SAGE-718, from 0.01 to 100 μM in log increments. To avoid cumulative effects of contamination by the compound penetrating the cell, a single oocyte was used for each measurement. For co-agonists studies, oocytes expressing GluN1/2A were used. Examining the effects of SAGE-718 on the glutamate concentration activation curve was performed by evoking currents with 10 μM of glycine and escalating concentrations of glutamate, from 0.1−100 μM in log increments. The co-application of 10 μM of glycine and escalating concentrations of glutamate was repeated a second time in the presence of 10 μM of SAGE-718. To study the effect of SAGE-718 on the concentration activation curves of other co-agonists, cells were first assessed in control conditions without SAGE-718 and in a presence of 100 μM of glutamate and escalating concentrations of glycine or D-serine (0.1–10 μM in log increments). Next, cells were exposed to a fixed concentration of SAGE-718 (10 μM) and escalating concentrations of the co-agonists (same range as control condition: 0.1–10 μM of glycine or D-serine). Currents within a single recording were normalized to max amplitude in the presence of the agonists and absence of SAGE-718. Data were captured using a HiQScreen propriety data acquisition (Multichannel Systems Reutlingen, Germany) and analysed by a script running on MATLAB (MathWorks, Natick, MA, USA). All experiments were carried out using at least four cells.

Acute slice whole-cell patch-clamp electrophysiology

Animal care and experimental procedures were performed in accordance with the UK Animals (Scientific Procedures) Act of 1986 incorporating European Directive 2010/63/EU on the protection of animals used for scientific purposes. Animal studies are reported in compliance with the ARRIVE guidelines (Percie du Sert et al., 2020) and with the recommendations made by the *British Journal of Pharmacology* (Lilley et al., 2020). Male Sprague–Dawley rats (6–8 weeks old) were housed in a temperature-controlled room on a 12:12-h light/dark cycle with food and water available ad libitum. Only male rats were used for this study because the primary goal was to evaluate primary pharmacology at NMDA receptors, and sex differences were not considered.

Animals were deeply anaesthetized with isoflurane and then decapitated, and the brain was removed. Coronal slices containing the striatum (350–400 mm) were cut using the VT1000S vibratome (Leica Biosystems, Buffalo Grove, IL, USA) in ice-cold artificial cerebrospinal fluid (aCSF) containing (in mM) 127 NaCl, 1.9 KCl, 1.2 KH_2PO_4, 2.4 $CaCl_2$, 1.2 $MgCl_2$, 26 $NaHCO_3$ and 10 D-glucose, 310–315 mOsm, bubbled with 95%/5% O_2/CO_2. Slices were maintained at room temperature. For recording, slices were transferred to a recording chamber continuously perfused with aCSF at a rate of 3–5 ml·min^{-1} at room temperature. Whole-cell patch-clamp recordings were performed on striatal neurons using the 'blind' technique. Thin-walled borosilicate glass recording pipettes with a resistance of 5–8 MΩ were filled with internal solution containing (in mM) 140 KGlu, 1 EGTA-Na, 10 HEPES, 4 Na_2ATP and 0.3 NaGTP, 305–310 mOsm, pH 7.3. A bipolar stimulating electrode was placed in the corpus callosum to stimulate corticostriatal glutamatergic inputs. NMDA receptor-mediated excitatory postsynaptic potentials (EPSPs) were pharmacologically isolated in Mg^{2+}-free aCSF (same as above but with no $MgCl_2$) supplemented with **AMPA receptor** antagonist **NBQX** (10 μM), $GABA_A$ receptor antagonist **GABAzine** (10 μM), **$GABA_B$ receptor** antagonist CGP55485 (400 nM) and 0.01% Kolliphor EL. NMDA receptor EPSPs were evoked every 30 s at a resting membrane/holding potential between −70 and −80 mV, and the target amplitude at baseline was 4–8 mV. Following stabilization of the baseline NMDA receptor EPSP, increasing concentrations of SAGE-718

were perfused onto the slice, from 10 nM to 10 μM in log increments. Each concentration was applied for 20 min. At the end of the experiment, D-APV (d-AP5; 20 μM) was perfused onto the slice to confirm the NMDA receptor-evoked EPSPs.

Data were acquired at 20–100 kHz using a MultiClamp 700B amplifier and an Axon Digidata 1550B digitizer controlled by pClamp Clampex 9 software (Molecular Devices, San Jose, CA, USA). EPSPs were averaged over the final 12–16 consecutive episodes for each condition during a recording, and the mean peak amplitude for each test article concentration was normalized to baseline peak amplitude. The half-decay time was measured manually from the peak response to half of the peak EPSP amplitude.

2.1.3 | Multi-electrode array (MEA)

Experiments and data analyses were performed as previously described (Gramowski-Voß et al., 2015; Hammond et al., 2017). All animal care and experimental procedures were carried out in accordance with the EU Directive 2010/63/EU on the protection of animals used for scientific purposes (certification file number 7221.3-2) and the German Animal Protection Act §4. Timed-pregnant NMRI mice were purchased from Charles River Laboratories (Sulzfeld, Germany). At Embryonic Day 15/16, the pregnant mice were killed by cervical dislocation and the embryo pups were decapitated. Primary frontal cortex tissues from the pups were collected and plated on poly-D-lysine and laminin-coated multi-electrode arrays (MEAs; Axion Biosystems).

Cultures were incubated at 37°C in a 10% CO_2 atmosphere and maintained in DMEM containing 10% horse serum, with 48 h of treatment with 5-fluoro-2′-deoxyuridine (25 μM) and uridine (63 μM) on Day 5 to prevent glial proliferation. Multichannel recordings were collected with the Plexon system (Dallas, TX, USA) using electrode MEA neurochips provided by the Center for Network Neuroscience (CNNS) at the University of North Texas. Recordings were performed on cultures at 27–34 days in vitro, and a stable activity pattern was established for 4 weeks. Recordings were made at 37°C in DMEM/10% heat-inactivated horse serum. Signals were sampled at 40 kHz and were recorded in a range of 15–1800 μV. Spike bursts were quantified with NeuroExplorer (Plexon Inc., Dallas, TX, USA) and NPWaveX (NeuroProof GmbH, Rostock, Germany). Bursts were defined by the beginning and end of short spike events. A measure of burst synchronicity (SynAll) was defined as the average distance of individual bursts within a population burst from the population burst centre. To assess the relative effect of SAGE-718 on burst synchronicity, the change in SynAll was normalized to the change in spike rate. The normalization corrects for the fact that a reduction in spike rate can increase individual burst duration and thus impact apparent burst synchronicity. To examine the effects of SAGE-718 on cultures, eight cumulatively increasing concentrations were administered after recording the native activity profile of the individual cultures. The analysis of the network activity was characterized in four categories: spike rate, burst duration, inter-burst interval (IBI) and SynAll. All compound-induced network activity was normalized to the related spontaneous native activity, set at 100% for each experiment. Values were derived from 60-s bin data taken from a 30-min span after a 30-min stabilization of activity, and data are presented as mean ± SEM.

2.2 | In vivo pharmacokinetics in rats

2.2.1 | Animal dosing

These experiments were carried out at ChemPartner. Co. Ltd., Shanghai, China. Animal care and experimental studies complied with the relevant protocols which were reviewed and approved by the Institutional Animal Care and Use Committee at ChemPartner. All procedures in this protocol were in compliance with local animal welfare legislation, ChemPartner policies and procedures, national standards GB14925, Euthanasia AVMA guidelines and the Guide for the Care and Use of Laboratory Animals. Male Sprague–Dawley rats (210-240g; supplied by the Shanghai Laboratory Animal Center [SLAC], Shanghai, China) were given a single i.p. dose of SAGE-718 (10 $mg \cdot kg^{-1}$) formulated in 30% Captisol (sulfobutylether-β-cyclodextrin). Male rats were used in this initial study to enable pharmacodynamic experiments; male and female pharmacokinetics (PK) experiments were conducted in a later stage of non-clinical development. Animals were had access to food and water ad libitum. Three animals were anaesthetized with inhaled isoflurane (2-3%) and then killed by cardiac puncture for blood collection, per time point (1, 4, 8, 12, 24, 48 and 72 h post dose). A 150-μl aliquot of whole blood was collected via cardiac puncture and, within 15 min of collection, was centrifuged at 2000 g for 5 min at 4°C to obtain plasma. Brain was collected, rinsed with cold saline and immediately snap frozen at −70°C until analysis.

2.2.2 | Sample preparation and bioanalysis

Brain tissues from untreated (control) rats and from animals dosed with SAGE-718 were first homogenized in 3:1 (v/w) PBS. Standard calibrators and quality control plasma and brain homogenate samples were prepared by adding SAGE-718 solutions (in DMSO) of known concentrations.

A 30-μl aliquot of plasma or brain homogenate sample was extracted via protein precipitation by addition of 100 μl of internal standard solution in acetonitrile (ACN). The mixture was vortex-mixed for 10 min and centrifuged at 5228 x *g* for 10 min. The supernatant was transferred to a 96-well plate for liquid chromatography tandem mass spectrometry (LC–MS/MS) analysis.

A 10-μl aliquot of supernatant was injected into an API5500 QTrap (Sciex, Framingham, MA, USA) coupled with an Acquity UPLC system (Waters, Milford, MA, USA) using electrospray positive ionization mode, monitoring mass transitions for SAGE-718 and internal standard. Plasma and brain concentrations were measured against standard calibration curves in each respective matrix.

Actual PK values are reported for studies where terminal samples were collected at the end of the experiments. Estimated PK values are reported for experiments where animals were not killed at the time of the behavioural testing and are extrapolated from definitive PK experiments that were completed during the preclinical development of SAGE-718. The methods for the definitive PK experiments were identical to those employed in the current experiments.

2.3 | In vivo pharmacology

2.3.1 | PharmacoEEG

This study was conducted in an Association for Assessment and Accreditation of Laboratory Animal Care (AAALAC)-approved facility (ChemPartner. Co. Ltd., Shanghai, China), under relevant protocols that were reviewed and approved by the vendor's Institutional Animal Care and Use Committee (see section 2.2.1). Male Sprague–Dawley rats (SLAC; 250–350 g; n = 12 per group) were singly housed under controlled conditions (temperature of 20–26°C, humidity of 40%–70% and 12:12-h light/dark cycle). Water and standard chow diet were available ad libitum. Animals were acclimated for 1 week to these conditions prior to electroencephalogram (EEG) implantation surgery. Male rats were used for this study as experimental parameters, such as ketamine doses required to modulate EEG, were previously validated in rats of this sex.

Rats were anaesthetized with 30 $mg \cdot kg^{-1}$ of zoletil and 3 $mg \cdot kg^{-1}$ of xylazine for electrode implant surgery. Two epidural recording electrodes were implanted (negative at +2.0 mm AP, −1.5 mm ML from bregma, and positive at −5 AP, +2.5 mm ML from bregma). An additional ground electrode was implanted over the cerebellum, and electromyography (EMG) electrodes were embedded in the cervical trapezius muscle. Electrodes were connected to a head stage that was cemented to the skull using dental acrylic. Rats were administered antibiotic (ceftriaxone sodium, 100 $mg \cdot kg^{-1}$, ip; Shanghai Xinya Pharmaceutical Gouyou Co., Ltd, Shanghai, China) and analgesia (buprenorphine, 0.3 $mg \cdot kg^{-1}$, ip; TIPR Pharmaceutical Responsible Co., Ltd, Tianjin, China) immediately after surgery. Rats were placed on a thermal pad (35°C) until regaining normal posture. Rats were allowed 1 week of recovery prior to EEG recordings.

For EEG recordings, rats were acclimated to the recording chamber (35 × 35 × 30 cm) for at least 45 min prior to 2 h of continuous EEG recording to establish baseline. Following baseline recording, each rat was injected with either SAGE-718 (1, 3 or 10 $mg \cdot kg^{-1}$, ip) or vehicle (30% Captisol + 0.01% Tween 80), and then continuous EEG was recorded for 6 h. Next, all rats received injections of ketamine (15 $mg \cdot kg^{-1}$, ip), and then continuous EEG was recorded for an additional 2 h. EEG was recorded using A-M Systems Differential AC Amplifier (Model 1700) and CED Micro 1401 with Spike 2 (Version 7.0, CED, Cambridge, UK). EEG recordings took place from a subset of rats, balanced across groups, each day for seven consecutive days. Recordings always began at a similar time each day, and the recording order with each day was also balanced across groups. At the end of the experiment, animals were killed by asphyxiation with CO_2, followed by cardiac puncture to collect blood.

EEG and EMG signals were digitized at a sampling rate of 512 Hz and band-pass filtered (0.1–500 Hz) with 50 Hz of notch filter off. The power spectrum was computed using fast Fourier transform (FFT) across time with sections of length 10 s and a Hanning window. EEG power was measured in the following frequencies: delta, 1–6 Hz; theta, 6–9 Hz; alpha, 9–13 Hz; beta, 13–30 Hz; gamma 1, 30–47 Hz; and gamma 2, 53–70 Hz. For each 10-s epoch of the recording, rats were characterized as waking or sleeping using SleepSign software (Kissei Comtec Co., Japan) combined with manual inspection, with wake defined based on a combination of EMG power (sleep corresponding to EMG power below an empirical threshold) and EEG power (sleep defined as delta power or theta/delta ratio above an empirical threshold). Changes in EEG power were normalized to the pre-injection baseline period to correct for baseline differences in EEG power across rats, which are standardly observed. Baseline-normalized changes in EEG power were plotted in 1-h bins and were calculated separately using data only from the wake state and sleep state or using all data without wake and sleep separation. For inclusion in separate wake and sleep analyses, each rat was required to spend a minimum of 5 min per 1-h bin in the respective wake or sleep category.

2.3.2 | Phencyclidine (PCP)-induced deficits in social interaction (SI) model (PCP SI)

This study was conducted under EU and French animal welfare regulations for animal use (European Directive 2010/63/EEC and French decree and orders of 1 February 2013) and was approved by the laboratory's ethics committee. Male Long-Evans rats (Janvier Labs, France; 160–220 g; n = 105; 12–15 per dose) were housed in groups of two to four animals with water and food ad libitum on a light/dark cycle of 12/12 h. Male rats were used for this study, as experimental parameters were validated using male rats only. The study was designed to generate groups of equal size, with randomization used to allocate animals to treatment groups. Rats were allowed to acclimate to environmental conditions for at least 5 days prior to experimentation in the SI test. Rats were treated with either 0.9% saline or 5 $mg \cdot kg^{-1}$ of PCP by i.p. injection twice daily (morning and afternoon) from Days 1 to 7. From Days 8 to 14, animals were housed in their home cages without any treatment. On the day prior to SI testing (from Day 13), rats underwent a 10-min habituation session, where they were allowed to freely explore the testing arena (90 × 90 × 40 cm of square wooden box) in a dark room (approximately 60 lux). Animals were habituated to the testing room for at least 30 min prior to testing. On the experimental day (starting on Day 14), rats were administered vehicle (30% Captisol + 0.1% Tween 80) or SAGE-718 (0.3, 1, 3 or 10 $mg \cdot kg^{-1}$) by i.p. injection (5 $mg \cdot ml^{-1}$) 60 min prior to the SI test. Treated rats were placed with a partner animal (age-matched, socially unfamiliar male Long-Evans rats) in the arena for a 10-min session (testing between 9:00 AM and 1:00 PM;

during the light phase). Time spent in SI was scored by an experimenter blind to drug treatment. SI was defined as non-aggressive social behaviour such as sniffing, following, grooming, kicking, mounting, jumping on, wrestling and crawling under and over the partner. All experimental groups were represented on each experimental day. SAGE-718 drug concentrations in plasma and brain were determined in satellite rats (n = 3 per group). At the end of the experiment, animals were killed with an overdose of pentobarbital (160 mg·kg^{-1}, i.p.).

2.3.3 | AY9944 studies

These studies were carried out at ChemPartner. Co. Ltd., Shanghai, China, in conditions fully compliant with the relevant protocols and regulations (see section 2.2.1). Sixteen timed pregnant female Sprague–Dawley rats were obtained from SLAC. The arrival date of the animals was counted as P0. The rats were housed under controlled conditions (temperature of 21.0 ± 2°C, humidity of 40%–70% and 12:12-h light/dark cycle with lights on at 5:00 AM). Water and normal chow diet were available ad libitum. Pups were housed with their mothers until P21 and then group housed by sex for the remainder of the study. The pups received a series of subcutaneous (s.c.) injections of AY9944 or physiological saline every 6 days from P2 to P86. Siblings from the same mother received the same treatment (either AY9944 [7.5 mg·kg^{-1}] or 0.9% saline, administered s.c.). For locomotor testing, females were used as they demonstrated the most robust alterations in activity during pilot testing, and the males were used for EEG recordings.

Locomotor activity testing

The female rats used in these experiments were the females that had been were born in-house (see section 2.3.3 above) and locomotor activity testing was carried out between P69-P76. The rats were placed individually in clean testing cages with free access to food and water. All rats were allowed to habituate to the testing room/cages for 30 min before compound administration. Animals (n = 12–23 per group) were removed from the home cage and injected with SAGE-718 (3 or 20 mg·kg^{-1}, i.p.) and placed back in the home cage for 180 min. At 180 min after dosing with compounds, each rat was placed in the testing cages that were mounted into a LABORAS (Metris Systems) behavioural recording system that codes vibrations/movements into behavioural outputs for continuous non-video-based monitoring. Rats were continuously monitored for an additional 180 min after compound administration. The digital signals were processed offline to classify spontaneous activity into seven categories: rearing, eating, drinking, climbing, immobility, grooming and circling. At the end of the experiment, animals were killed by asphyxiation with CO_2, followed by cardiac puncture to collect blood.

Surgery for EEG recordings in the AY9944 studies

Head stage electrodes were implanted in male rats (see section 2.3.3. above), 10–14 days before EEG recordings, at P62–P69. Body weights were taken, and rats were anaesthetized with sodium pentobarbital (60 mg·kg^{-1}, 2 ml·kg^{-1}, i.p.). The head was shaved, and the rat was securely mounted in a stereotaxic frame. The scalp was cleaned with 75% ethanol and medical iodine prior to making a 2- to 2.5-cm incision followed by application of 3% hydrogen peroxide to remove the membrane surrounding the skull and identification of bregma. Two frontal and two parietal monopolar epidural electrodes were surgically implanted at the following coordinates: 3 mm lateral from midline and 2.2 mm anterior or posterior to bregma for the two frontal or parietal electrodes, respectively. An additional ground electrode was inserted towards the back of the skull over the cerebellum. Four screws were then inserted, electrode wires were tightly wound around each of their respective electrodes, and the head stage and all electrode wires were secured with dental cement to the skull. The scalp was then sutured, and all rats were treated with benzylpenicillin sodium (30 mg·kg^{-1}, i.p.) and the analgesic **carprofen** (5 mg·kg^{-1}, s.c.).

Electrocorticogram (EcoG) recordings

The EcoG recordings were taken from unrestrained animals (n = 9–20 per group) that were placed in individual recording chambers for a 15-min adaptation period prior to the baseline recording to minimize movement artefacts. Each rat was recorded continuously for a 2-h baseline EEG. All drugs were administered i.p. to each rat immediately after the 2-h baseline. Following compound administration, each rat was recorded continuously for four additional hours for a total continuous recording duration of 6 h. Video was recorded during the 6 h of EEG recording. The EcoG signal was band-pass filtered (2.6–96 Hz) and processed with Spike 2 software to automatically recognize sharp wave discharges (SWDs). AY9944-induced absence seizures were quantified by measuring the total duration and number of SWDs for every consecutive 30-min epoch over the 6-h recording period. SWD in the ECoG was identified as 4–6 Hz of activity, amplitude of at least 1.6-fold higher than baseline, inter-spike intervals > 0.25 s and number of spikes in an SWD train > 4. At the end of the experiment, animals were killed by asphyxiation with CO_2, followed by cardiac puncture for blood collection.

Determination of plasma cholesterol and 24(S)-HC in plasma and brain, using LC–MS/MS

The LC system comprised a Shimadzu (Shimadzu Co., Japan) liquid chromatography equipped with a binary pump (LC-30AD), an autosampler (SIL-30AC), a column oven (CTO-20A), a system controller (CBM-20A) and a degasser (DGU-20A). Mass spectrometric analysis was performed using an AB SCIEX API6500+ triple-quadrupole (Ontario, Canada) instrument with an electrospray ionization (ESI) interface. The data acquisition and control system was equipped with Analyst 1.6.2 software from AB SCIEX.

Chromatographic separation was on a C18 column (Waters BEH C18; 2.1 × 50 mm, 1.7 μm), where mobile phase A was water (containing 0.05% formic acid [FA]) and mobile phase B was ACN (containing 0.05% FA). The column was eluted at a flow rate of 0.5 ml·min^{-1} in a gradient programme consisting of 5% phase B (0–0.3 min), from 5% to 45% B (0.3–1.0 min), from 45% to 80% B (1.0–3.50 min), 80% B (3.50–6.00 min), from 80% to 5% B (6.00–6.01 min) and 5% B

(6.01–7.50 min). For 24(S)-HC, the retention time for the analyte and IS (SGE-102) was 3.70 and 2.76 min, respectively; the injection volume was 3 µl. The precursor product ion pair was m/z 367.2 → 147.2 for 24(S)-HC and m/z 319.1 → 283.3 for SGE-102.

Standard curve preparation

Stock solutions of 24(S)-HC were prepared at 1 mg·ml^{-1} in DMSO. The stock solution was diluted with MeOH to prepare serial working solution (60, 100, 200, 600, 2000, 6000, 20,000, 60,000 and 2,000,000 ng·ml^{-1}), and an aliquot of 10 µl of working solution was added to 190 µl of PBS to obtain calibration standard curve (3, 5, 10, 30, 100, 300, 1000, 3000 and 10,000 ng·ml^{-1}).

Sample preparation

The brain tissues were homogenized for 2 min with 3 volumes (v/w) of homogenizing solution (PBS). An aliquot of 10 µl of brain homogenate sample was diluted with 90 µl of PBS. An aliquot of 30 µl of sample (plasma or brain homogenates) was added to 150 µl of IS (IS-102, 200 ng·ml^{-1}) in ACN. The mixture was vortexed for 5 min and centrifuged at 20,817 x g for 5 min. An aliquot of 3 µl of supernatant was injected for LC–MS/MS analysis.

2.3.4 | Pentylenetetrazole (PTZ) infusion seizure model

This study was conducted at Melior Discovery Inc. (Exton, PA. USA), in an AAALAC-approved facility with Office of Laboratory Animal Welfare (OLAW) assurance under relevant protocols that were reviewed and approved by the Institutional Animal Care and Use Committee. Male CD1 mice (8–10 weeks of age; Charles River Laboratories, Kingston, NY, USA) were group housed (no more than four mice per cage) on a 12-h light/dark cycle (lights on at 7:00 AM) and acclimated for at least 3 days prior to evaluation. Male mice were used for this study, as experimental parameters were validated for male mice only. The study was designed to generate groups of equal size, with randomization used to allocate animals to treatment groups. Mice were acclimated to the procedure room for at least 30 min. Mice were restrained in hard plastic restrainers, and PTZ (Sigma-Aldrich, St. Louis, MO, USA; 10 mg·ml^{-1} formulated in dH_2O) was infused intravenously (i.v.) with a syringe pump at 0.3 ml·min^{-1} via a butterfly cannula placed in a superficial tail vein, with a cut-off of 2 min. On the day of PTZ seizure assay, mice (n = 14–15 per group) were treated (i.p., 10 ml·kg^{-1}) with vehicle (30% SBECD + 0.01% Tween 80), SAGE-718 (10, 30 and 50 mg·kg^{-1}) or theophylline (120 mg·kg^{-1}; formulated in dH_2O) or orally (p.o.) with diazepam (10 mg·kg^{-1}; formulated in 0.5% MC:0.2% Tween 80) and subsequently assessed for PTZ seizure threshold, 30 min (diazepam and theophylline) or 4 h (SAGE-718 and vehicle) prior to PTZ administration. Latency to onset of a myoclonic twitch/running–bouncing clonus and tonic hindlimb extension seizure was recorded during the 1-day study duration by an experimenter who was blinded to the treatment groups. One mouse of the theophylline group died between dosing and PTZ evaluation. One mouse in each 30 mg·kg^{-1} of SAGE-718, 50 mg·kg^{-1} of SAGE-718 and diazepam group was excluded due to a technical issue. Immediately after the PTZ seizure assay, animals were killed using isoflurane, followed by cardiac puncture for blood collection and then cervical dislocation. Plasma and brain samples were collected from three animals per drug-treated group.

2.4 | Chronic rat toxicity

This study was conducted at Charles River Laboratories (Ashland, OH, USA) in AAALAC-accredited facilities. The protocol and amendments were approved by the CRL Ashland IACUC committee and complied with all applicable sections of the Final Rules of the Animal Welfare Act regulations (Code of Federal Regulations, Title 9), the Public Health Service Policy on Humane Care and Use of Laboratory Animals from the Office of Laboratory Animal Welfare (Office of Laboratory Animal Welfare, 2015), and the Guide for the Care and Use of Laboratory Animals from the National Research Council, 2011. Sprague Dawley rats (Crl:CD(SD)) were supplied by CRL (Raleigh, NC). The rats were approximately 8 weeks old and weighed 175-267 g for male rats and 144-211 g for female rats, on day 1 of dosing.

The potential toxicity of SAGE-718 was evaluated in a 6-month rat toxicity study where SAGE-718 was administered once daily via oral gavage to groups of male and female rats at dose levels of 0.8, 2.5 and 7 mg·kg^{-1}·day^{-1} to male rats and 2, 6 and 15 mg·kg^{-1}·day^{-1} to female rats. All doses were formulated in 20% hydroxypropyl-β-cyclodextrin (HPβCD) in deionized water and administered at a dose volume of 4 ml·kg^{-1}. A separate group of male and female rats was used as a control group and received once daily doses of the vehicle (20% HPβCD in deionized water). All animals were observed at least once daily for clinical signs, and body weights and food consumption were recorded weekly. Plasma samples for toxicokinetic analysis were collected from satellite animals on Days 1, 91 and 182. Following the completion of the dose administration period, the main study rats were killed by asphyxiation with CO_2 and a full set of tissues, including eight transverse sections of the brain, were collected, embedded in paraffin, sectioned, mounted on glass slides and stained with haematoxylin and eosin for microscopic analysis. The full set of tissues were examined from the control and high-dose animals, and gross lesions and target tissues were examined for the low- and mid-dose animals and animals assigned to the recovery necropsy.

2.5 | Data and statistical analysis

The data and statistical analysis comply with the recommendations of the *British Journal of Pharmacology* on experimental design and analysis in pharmacology (Curtis et al., 2022). For all experiments, *P*-values < 0.05 were considered statistically significant. Declared group size in individual studies reflects the number of independent values (n) that were used for statistical analysis; where n<5, data are exploratory and were not subjected to statistical analysis. In multigroup

studies with parametric variables, post hoc tests were conducted only if the analysis of variance (ANOVA) achieved statistical significance ($P < 0.05$) and there was no significant variance in homogeneity.

2.5.1 | In vitro electrophysiological experiments

Concentration–response curves were generated by fitting the data normalized to baseline or vehicle peak current amplitude with a four-parameter logistic curve fit with the bottom constrained to 0 and the Hill slope limited to a maximum of 2 using least squares regression (GraphPad Prism Version 8, San Diego, CA, USA). Potency (half maximal effective concentration [EC_{50}]) and efficacy (maximal efficacy [E_{max}], percentage change from baseline) were derived from curve fits with a symmetrical approximate 95% confidence interval (CI). When appropriate, the concentration–response curves were compared by the extra-sum-of-squares *F* test, using $LogEC_{50}$ to measure the difference between datasets. For the ketamine inhibition kinetics experiment, statistical significance between vehicle and SAGE-718 blocking kinetics was assessed with a two-way mixed ANOVA using Bonferroni's correction for multiple comparisons. For the acute slice electrophysiology experiment, peak amplitude (in millivolts) and half decay (in milliseconds) were analysed using a mixed-effects restricted maximum likelihood (REML) model with Geisser–Greenhouse's correction and Dunnett's multiple-comparisons test to compare each test concentration to baseline control. The mixed-effects model was used instead of repeated-measures ANOVA because one cell was not evaluated against all test concentrations. For the MEA experiment, the effects of SAGE-718 versus vehicle were analysed using two-way ANOVA and Bonferroni's multiple-comparisons tests.

2.5.2 | In vivo pharmacology experiments

For the pharmacoEEG experiment, changes in frequency band power were analysed using two-way ANOVA (SAGE-718 dose × time) with post hoc Dunnett's test. A secondary analysis was performed on a finer time scale to examine effects of the ketamine challenge on frequency oscillations in the gamma band and was designed specifically to address return to previous state of the EEG at the level of the individual animal. For each rat, the power spectrum was computed as a function of time using multitaper spectral methods (Multitaper Toolbox; Prerau et al., 2017). The parameters for the multitaper analysis were window length T = 10 s with no overlap, time-bandwidth product TW = 5 and number of tapers K = 9. Sections of EEG reported to be recorded during sleep were removed. At each resulting 10-s time bin, the gamma 1 band was computed as the average signal between 31 and 47 Hz and the gamma 2 band as the average signal between 53- to 70-Hz. To reduce noise in the signal, the time series was then smoothed using a 10-min rolling mean. Time to return to pre-ketamine levels was computed as follows. For each rat, the mean and standard deviation in each gamma band level were estimated in the 2-h period before ketamine challenge. Time to return to pre-level was then computed as the time between application of ketamine and the time for the mean EEG power to return to 2 standard deviations above this initial mean value. The motivation of a choice of a slighter higher threshold than the original mean was to generate slightly higher likelihood of getting an actual return time rather than having the return data censored at 2 h, when the experiment was stopped. Comparison of return times as a function of dose was performed using Cox proportional hazards regression (R package, Version 4.1.1, survival_3.2-11).

For the PCP SI study, SI time from all animals was analysed using SAS software with the following comparisons: (1) vehicle (Veh)/saline versus Veh/PCP using a two-tailed Student's *t* test to demonstrate PCP-induced social deficit and (2) comparison of Veh/PCP versus doses of SAGE-718/PCP using a one-way ANOVA with a post hoc Dunnett's test to determine an effect of SAGE-718 on PCP-induced SI deficits.

To examine effects of SAGE-718 on locomotor activity and SWD in AY9944- and vehicle-treated rats, one-way ANOVA was utilized to compare compound treatment relative to AY9944 treatment only, with post hoc Dunnett's analyses employed to examine pairwise comparisons. Simple linear regression was employed to examine the relationship between 24(S)-HC and locomotor activity. For EcoG recordings in AY9944- and vehicle-treated rats, *t* tests of means were utilized to examine differences between AY9944- and vehicle-treated animals.

For the PTZ seizure model, clonic and tonic latency data were analysed using GraphPad Prism, with the following comparisons: (1) Veh versus SAGE-718 using a one-way ANOVA followed by post hoc Dunnett's test (vs. vehicle control), (2) Veh versus diazepam using a Student's *t* test for clonic latency and a Mann–Whitney test for tonic latency and (3) Veh versus theophylline using a Student's *t* test.

2.6 | Materials

SAGE-718 was prepared as previously described (Hill et al., 2022). 24(S)-HC was prepared similarly as described previously (Zhang et al., 2002). Kolliphor EL and PTZ were obtained from Sigma-Aldrich. NBQX, GABAzine, CGP55485 and D-APV were obtained from Tocris (Abingdon, UK). Ketamine hydrochloride (Ketalar) was acquired from Pfizer (Surrey, UK) or Zhong Mu Bei Kang Pharmaceutical Co. Ltd. (Jiangsu, China). PCP was acquired from HPC Pharmaceuticals (Rennes, France). AY9944 dihydrochloride was acquired from Tocris (Minneapolis, MN, USA).

2.7 | Nomenclature of targets and ligands

Key protein targets and ligands in this article are hyperlinked to corresponding entries in http://www.guidetopharmacology.org and are permanently archived in the Concise Guide to PHARMACOLOGY 2021/22 (Alexander, Christopoulos et al., 2021; Alexander, Fabbro et al., 2021; Alexander, Mathie, et al., 2021).

3 | RESULTS

3.1 | SAGE-718 is a neuroactive steroid NMDA receptor PAM

SAGE-718 was evaluated for effects on NMDA receptor activity, using recombinant GluN1/GluN2 subtypes expressed in HEK293 cells on the IWB automated patch-clamp platform. NMDA receptor currents were activated by EC_{20} glutamate (0.8 μM) and maximal glycine (30 μM). The potency (EC_{50}) and efficacy (E_{max}) of SAGE-718 on GluN1/GluN2 subtypes have been previously reported (Hill et al., 2022). SAGE-718 potentiated co-agonist evoked NMDA receptor currents on all GluN1/2 subtypes in a dose-dependent manner with higher efficacy levels on 2A and 2B (n = 8 per group) (Figures 1b and S1). In an assessment of GluN1/2A-2D on *Xenopus* oocytes using TEVC, SAGE-718 potentiated currents on the four di-heteromeric GluN1 and GluN2 subunit combinations with near equivalent efficacy (Figure S2A). In a manual whole-cell patch-clamp study on GluN1/GluN2A recombinantly expressed in HEK293 cells, SAGE-718 potentiated NMDA receptor currents evoked with submaximal NMDA (30 μM) and glycine (5 μM) (Figure 1c). SAGE-718 produced similar levels of potentiation on GluN1/GluN2A from human, mouse, rat and dog (Figure S2B). Because some neuroactive steroids, such as pregnenolone sulfate, modulate both NMDA and $GABA_A$ receptors (Akk et al., 2001; Wu et al., 1991), SAGE-718 activity was evaluated on $GABA_A$ receptor subtypes α1β2γ2 and α4β3δ, stably expressed in Ltk and transiently transfected in CHO cells, respectively, using manual patch clamp. SAGE-718 potentiated $GABA_A$ receptor α1β2γ2 currents evoked by submaximal GABA (2 μM), with an EC_{50} of 570 nM (95% CI, 270–1200) and an E_{max} of 310% potentiation over baseline (260%–360%), while having no effect on α4β3δ currents (Figure S3). These data show that SAGE-718 is a potent pan-selective PAM of NMDA receptors, with >10-fold selectivity over $GABA_A$ receptors α1β2γ2 subtype.

To evaluate activity in a more biologically integrated preparation, SAGE-718 activity was assessed on adult rat dorsal striatal medium

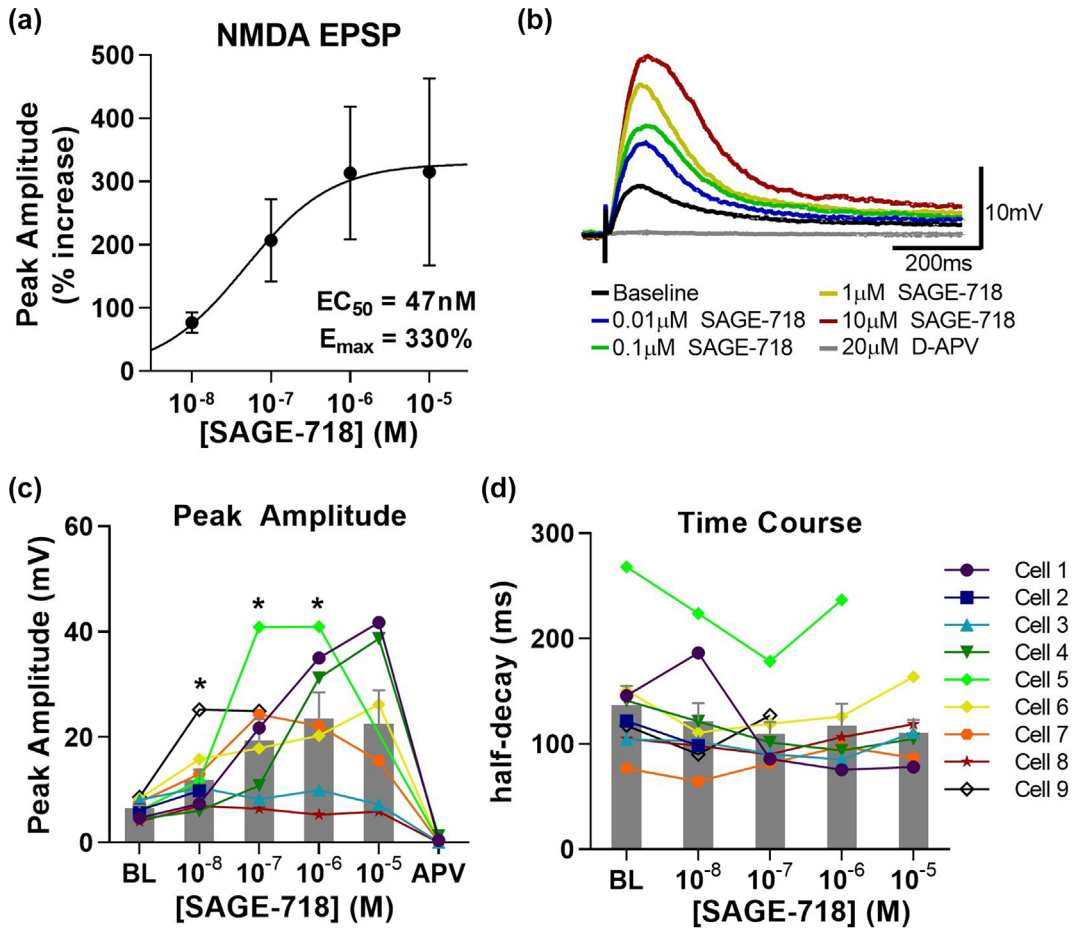

FIGURE 2 SAGE-718 potentiates evoked NMDA receptor excitatory postsynaptic potentials (EPSPs) in rat striatal medium spiny neurons. (a) Concentration–response of SAGE-718 potentiation of an evoked NMDA receptor EPSP (n = 9 neurons from 4 rats). EC_{50} = 47 nM (95% CI, 25-890); E_{max} = 330% (140-520). (b) Representative EPSP traces recorded from neurons at baseline and with 0.01, 0.1, 1 and 10 μM of SAGE-718 and 20 μM of APV. (c) Peak EPSP amplitude (millivolts) at baseline (BL) and each SAGE-718 concentration, for each individual cell (symbols) and mean (bars). Dunnett's multiple-comparisons test: $^*P < 0.05$, significantly different from baseline (BL). (d) Half-decay (in milliseconds) at BL and each SAGE-718 concentration.

spiny neurons in an acute slice brain preparation. SAGE-718 dose-dependently increased NMDA receptor EPSPs (Figure 2a). NMDA receptor EPSPs were fully blocked by application of d-AP5 (Figure 2b). SAGE-718 produced significant increases in EPSP amplitude at all concentrations except 10 μM, a concentration at which precipitation was evident (Figure 2c). SAGE-718 had no effect on EPSP half-decay time (Figure 2d). These results show that SAGE-718 has similar potency and efficacy on recombinantly expressed and native NMDA receptors.

3.2 | SAGE-718 mechanism of action

To evaluate the potential mechanism that underlies SAGE-718 activity, we measured the effect of 10 μM of SAGE-718 on the NMDA receptor co-agonist concentration–response relationship. In an exploratory study, SAGE-718 produced a leftward shift in the concentration–response curve in the three co-agonists, glutamate (n = 7), glycine (n = 4) and D-serine (n = 4) (Figure 3a–c and Table S1). In addition, SAGE-718 appeared to increase the NMDA

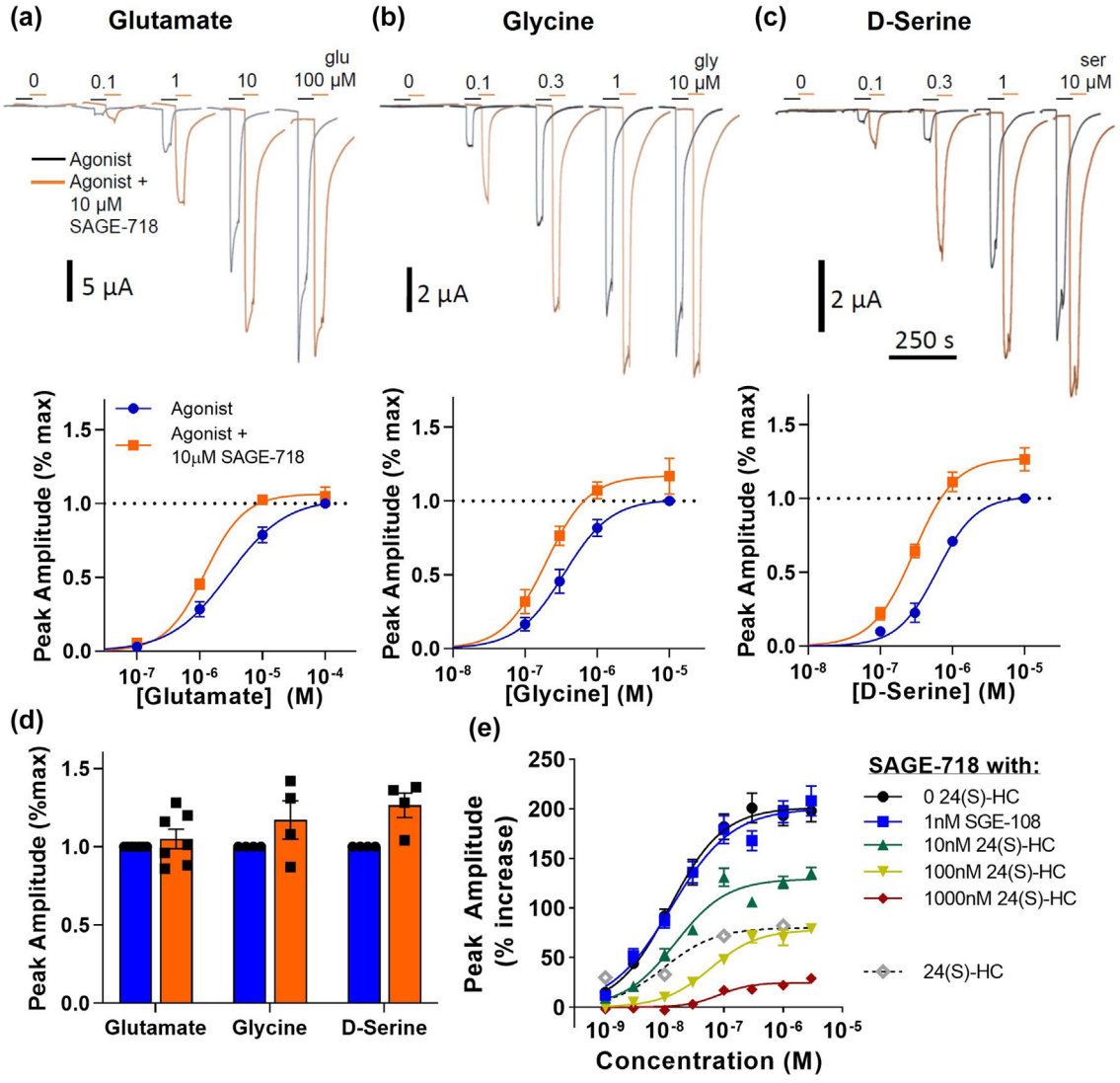

FIGURE 3 SAGE-718 increases the potency of endogenous NMDA receptor co-agonists. (a–c) Representative traces (top) and concentration–response relationship of NMDA receptor co-agonists (bottom) glutamate (a, n = 7 cells), glycine (b, n = 4 cells) and D-serine (c, n = 4 cells) in the absence (blue) or presence of 10 μM of SAGE-718. Two-electrode voltage-clamp configuration recordings conducted on oocytes expressing GluN1/GluN2A. NMDA receptor currents evoked by 10 μM of glycine (saturating) with increasing concentrations of glutamate (a) and 100 μM of glutamate (saturating) with increasing concentrations of glycine (b) or D-serine (c). Traces are shown offset to visualize peak current ± SAGE-718; bars indicate where agonist was added; SAGE-718 was continuously applied throughout experiment. (d) Summary of effects of 10 μM of SAGE-718 on peak amplitude evoked by maximal co-agonist, normalized to the peak current in the absence of SAGE-718. (e) Concentration–response curves of 24(S)-HC only (dotted line) and SAGE-718 on NMDA receptor currents in the absence or presence of 1, 10, 100 or 1000 nM of 24(S)-hydroxycholesterol (24(S)-HC).Whole-cell recordings conducted on HEK cells expressing GluN1/GluN2A and measured on the SyncroPatch automated platform. NMDA receptor currents evoked by 1 μM of glutamate (sub-saturating) and 100 μM of glycine (saturating). n = 3–8 wells per concentration. Data shown are means ± SEM.

receptor current at maximal D-serine (Figure 3d). These data suggest that SAGE-718 enhances the potency of the NMDA receptor endogenous co-agonists but only increases efficacy at maximal agonist concentration with D-serine.

The endogenous neuroactive steroid 24(S)-HC is a PAM of NMDA receptors and is dynamically regulated in the brain in a regionally specific manner (Popiolek et al., 2020). To evaluate whether SAGE-718 and 24(S)-HC share common structural determinants on NMDA receptors, the ability of 24(S)-HC to compete with SAGE-718 modulation was examined. 24(S)-HC, used alone, displayed potent PAM activity at NMDA receptors (EC_{50}, mean [95% CI] = 8.8 nM [4.3–18]; E_{max} = 80 [68–92] %; Figure 3e). When 24(S)-HC was added to the extracellular solution at 1000 nM, a concentration > 100× over the EC_{50}, SAGE-718 modestly potentiated NMDA receptor activity, and as 24(S)-HC levels were decreased, SAGE-718 efficacy increased (Figure 3e). These data suggest that SAGE-718 and 24(S)-HC are likely to bind to overlapping sites on GluN1/GluN2A.

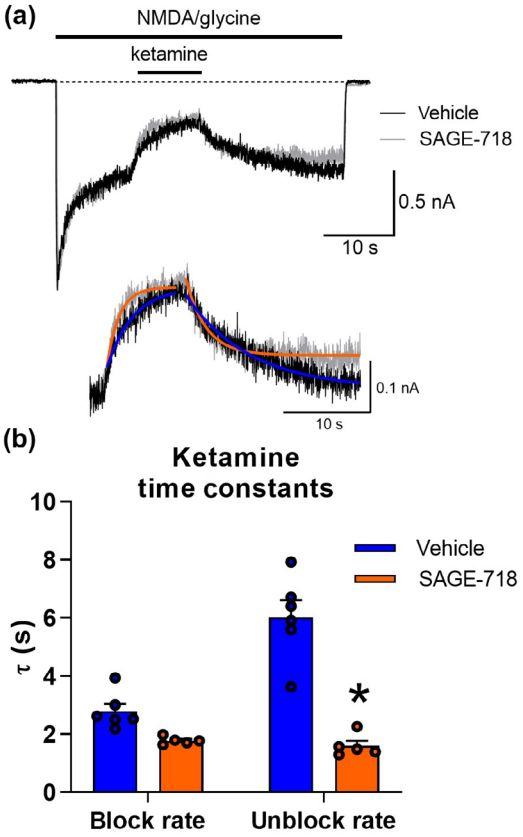

FIGURE 4 SAGE-718 accelerates the unblock rate of ketamine. (a) Top: Representative current trace from two HEK cells expressing GluN1/GluN2A in the absence or presence of SAGE-718 (10 μM). NMDA receptor current is evoked by 300 μM of NMDA (sub-saturating) and 100 μM of glycine (saturating) and then partially blocked by 0.6 μM of ketamine. The display traces were chosen because these two cells have similar current amplitudes, which enabled comparison of current decay and recovery in the presence and absence of ketamine. Bottom: Current trace during ketamine perfusion showing fit of block rate and unblock rate in the absence or presence of SAGE-718 (10 μM). (b) Summary of effect of SAGE-718 on block and unblock rates of ketamine. Data shown are means ±SEM from n = 5–6 cells. *$P < 0.05$, significantly different from vehicle; two –way mixed ANOVA with Bonferroni's multiple-comparisons test.

To further understand the mechanism by which SAGE-718 increases the activity of NMDA receptors, the rates of block and unblock by ketamine were evaluated in the presence and absence of SAGE-718. Because ketamine is an open channel blocker of NMDA receptors, altering the ketamine block and unblock rates would provide evidence that SAGE-718 can change the open probability of NMDA receptors (Linsenbardt et al., 2014; Orser et al., 1997). In addition, understanding the interaction between SAGE-718 and ketamine can be translated to both preclinical and clinical models of target engagement. NMDA receptor currents were elicited with 300 μM of NMDA and 100 μM of glycine in the presence or absence of 10 μM of SAGE-718. Ketamine (~IC_{50}, 0.6 μM) was applied after the NMDA receptor current amplitude began to reach a steady state (Figure 4a). The current decay during ketamine application and recovery following ketamine removal were each fit with a single exponential for vehicle and SAGE-718 conditions (Figure 4a). SAGE-718 significantly accelerated the rate of unblock by ketamine with a trend towards increasing the block rate (Figure 4b), suggesting that SAGE-718 increases the open probability of NMDA receptors similarly to other neuroactive steroid PAMs of these receptors (Linsenbardt et al., 2014). The extent of potentiation by SAGE-718 was not measured in these experiments due to differences in channel expression between cells.

We next evaluated whether SAGE-718 alters channel activity and block by ketamine in vivo. To determine dose selection, rat pharmacokinetics were first characterized. A single 10 mg·kg^{-1} i.p. administration of SAGE-718 in male SD rats resulted in sustained exposure through 72 h post dose in plasma and brain (Figure S4). Brain t_{max} was reached at 12 h post dose at a C_{max} of 2674 ng·g^{-1}, and brain-to-plasma ratio determined across 0–72 h was 5.31. Pharmacokinetic properties of this dose of SAGE-718 are summarized in Table 1. To determine the effects of SAGE-718 on ketamine in vivo, we measured the effects of SAGE-718 (1, 3 and 10 mg·kg^{-1}, ip) on EEG recorded from awake non-anaesthetized rodents, both prior to and following a ketamine challenge (15 mg·kg^{-1}, ip). EEG was

TABLE 1 Pharmacokinetic properties of SAGE-718 in male SD rats following 10 mg·kg^{-1} i.p. injection.

Matrix	t_{max} (h)	t_{last} (h)	C_{max} (ng·ml^{-1} or ng·g^{-1})	B:P C_{max}	Terminal $t_{1/2}$ (h)	AUC_{0-t} (h·μg^{-1}·ml^{-1})	B:P AUC_{0-t}
Plasma	1.0	72	1425	NA	26.3	20.6	NA
Brain	12	72	2674	1.88	30.7	109.5	5.31

Note: Data shown are derived from 3 rats per time point; parameters fit through mean concentrations at each sampling time point.
Abbreviations: AUC, area under the curve; B:P, brain-to-plasma ratio; i.p., intraperitoneal; NA, not applicable; SD, Sprague–Dawley.

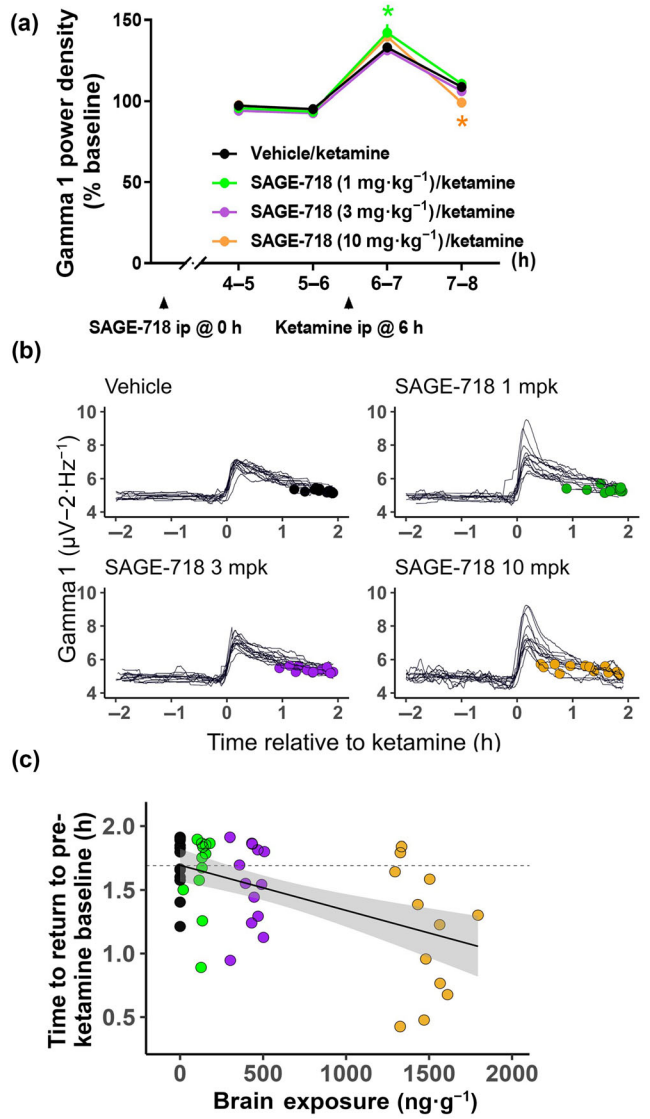

FIGURE 5 SAGE-718 boosts initial response to ketamine in gamma band and accelerates return to pre-ketamine at the highest dose. (a) Time course of wake electroencephalogram (EEG) power in the gamma 1 band (30–47 Hz) following administration of SAGE-718 and ketamine. EEG power density is normalized to the baseline recording before SAGE-718 injection and plotted in 1-h bins. Ketamine injection increased gamma power, which was enhanced by SAGE-718 (1 mg·kg^{-1}); 1–2 h after ketamine injection, SAGE-718 (10 mg·kg^{-1}) significantly decreased gamma power. Data are plotted as mean ± SEM for each group (n = 12–13 per group); error bars are within the size of the symbols for most data points. *P < 0.05, significantly different from Vehicle/Ketamine. (b) Wake time courses of raw, unnormalized gamma 1 band (31–47 Hz) for all rats in the pharmacoEEG study showing a 4-h time window centred around the injection of ketamine. Dots show the earliest time point where the signal returns to 2 standard deviations above the pre-ketamine signal. Mean time to return to pre-ketamine levels decreases with increasing dose of SAGE-718 and is significantly below vehicle for the highest 10 mg·kg^{-1} dose (Table S2). (c) After ketamine challenge, time to return to pre-levels decreases significantly as a function of brain exposure to SAGE-718 in rats (linear model, $R^2 = 0.26$, F[1,47] = 18.24, P < 0.05, beta = −3.55e-4). Key to different doses of SAGE-718 as in Figure 5a.

continuously recorded for 2 h prior to any injection and used to establish baseline EEG power. SAGE-718 had no detectable effect on EEG power in awake rats in any frequency band prior to ketamine injection (Figures S5 and S6). The ketamine injection caused a characteristic increase in gamma power (Kocsis, 2012). When analysed in broad (1 h) time bins, SAGE-718 caused a dose-dependent modulation of ketamine's effect on gamma power (Figure 5a). In the first hour after ketamine injection when its peak effect on gamma was observed, SAGE-718 at 1 mg·kg^{-1} enhanced the effect of ketamine on gamma 1 power. On the other hand, during the second hour after ketamine injection when gamma power is returning to baseline, SAGE-718 at 10 mg·kg^{-1} lowered gamma relative to ketamine alone.

Based on the observations above, a secondary analysis was performed on a finer time scale to examine effects of the ketamine challenge on frequency oscillations in the gamma band and was designed specifically to address return to previous state of the EEG at the level of the individual animal. Figure 5b shows the raw, unnormalized gamma 1 power estimated for each rat using multitaper spectral methods. Dots marked on each time course correspond to the first return time to a level that is 2 standard deviations above the signal before ketamine dosing. This return time was significantly higher at the 10 mg·kg^{-1} dose of SAGE-718 when compared with vehicle (Table S2). Figure 5c shows the relationship between time to return to pre-ketamine baseline and SAGE-718 brain exposure measured in the same animals 2 h after the ketamine challenge. There was a significant trend for faster return to baseline with increased brain exposure. A similar relationship was observed between the gamma 2 band and brain exposure (see Figure S7 and Table S3). These results are consistent with the accelerated recovery from ketamine block in vitro with SAGE-718 (Figure 4) and, importantly, also provide evidence that SAGE-718 modulates NMDA receptor function in vivo.

3.3 | SAGE-718 improves SI deficits produced by subchronic PCP administration

We next evaluated the activity of SAGE-718 in a preclinical model of NMDA receptor hypofunction. PCP administered daily for 7 days produces a range of behavioural deficits in rats including impaired SI (Grayson et al., 2007; Jenkins et al., 2008; Paul et al., 2013; Snigdha & Neill, 2008). We evaluated whether SAGE-718 could reverse SI deficits in rats administered subchronic PCP (PCP SI). Vehicle-treated rats previously administered PCP spent significantly less time in active SI than animals previously administered saline (Figure 6), indicating that subchronic PCP administration induced a social impairment. SAGE-718 (0.3, 1, 3 and 10 mg·kg^{-1}) increased SI time at all doses, compared with Veh/PCP-treated rats, with significant effects at 0.3, 1 and 3 mg·kg^{-1} (Figure 6). SAGE-718 plasma concentrations increased in a dose-dependent manner at 1, 3 and 10 mg·kg^{-1}, with concentrations within a range of 30–71 ng·ml^{-1} (n = 2; n = 1 below the level of quantification [BLQ]), 58–145 ng·ml^{-1} (n = 2; n = 1 BLQ) and 259 ± 104 ng·ml^{-1} (n = 3, mean ± SD), respectively. SAGE-718 brain concentrations were detectable at 3 mg·kg^{-1} (46 ng·g^{-1}; n = 1; n = 2

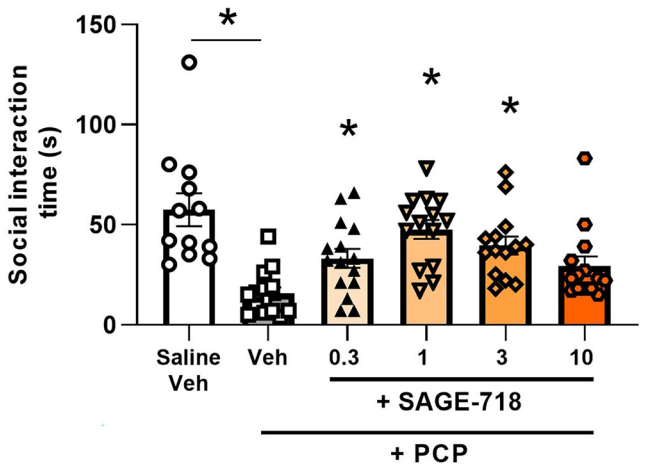

FIGURE 6 SAGE-718 increased social interaction (SI) time in the phencyclidine (PCP)-induced SI deficit model. Summary of effect of SAGE-718 (i.p., 60 min prior to SI test) on SI time in rats treated with PCP for 7 days followed by a 7-day washout period. Doses are expressed as mg kg^{-1}. Veh, vehicle. Data are shown as mean ± SEM from n = 12–15 animals per group. *$P < 0.05$, PCP significantly different from saline; Student's *t* test; or significant effect of SAGE-718 on PCP response; one-way ANOVA with Dunnett's test.

BLQ) and 10 mg·kg^{-1} (61 ± 11.1 ng·g^{-1}; n = 3). SAGE-718 levels were BLQ 1 h after i.p. administration in plasma at 0.3 mg·kg^{-1} and in brain at 0.3 and 1 mg·kg^{-1} in all satellite rats; the lowest level of quantification (LLOQ) was 10 ng·ml^{-1} in plasma and 40 ng·g^{-1} in brain. A minimally effective brain concentration range at 0.3 mg·kg^{-1} was extrapolated from the 3 and 10 mg·kg^{-1} doses and, therefore, was estimated to be 1.8–4.6 ng·g^{-1} (4–10 nM). At brain exposure levels associated with efficacy in the PCP SI model, the estimated NMDA receptor potentiation level with SAGE-718 was approximately 40% (EC_{10}–EC_{20}), while $GABA_A$ receptor coverage and potentiation were negligible (<10% potentiation), suggesting an on-target mechanism. Together, these data demonstrate that SAGE-718 improved social deficits induced by the NMDA receptor antagonist PCP.

3.4 | SAGE-718 attenuates behavioural manifestations of systemic cholesterol depletion

Cholesterol dysregulation is associated with a number of severe brain disorders (Vance, 2012). For example, Smith–Lemli–Opitz syndrome (SLOS) is caused by a mutation in the enzyme (7-dehydrocholesterol reductase) which converts 7-dehydrocholesterol to cholesterol, and is characterized by intellectual disability and a range of physical malformations (Nowaczyk & Irons, 2012). Low levels of 7-dehydrocholesterol reductase lead not only to reduced cholesterol levels but also decreased 24(S)-HC levels (Björkhem et al., 2001), which are likely to decrease NMDA receptor activity (Sun et al., 2016). We pharmacologically reproduced the decreased activity of 7-dehydrocholesterol reductase in SLOS, using subchronic administration of the enzyme inhibitor AY9944 (7.5 mg·kg^{-1}, s.c.; once daily every 6 days from Post-natal Day 2). Subchronic treatment with AY9944 produces SWDs (Figure 7a), and in AY9944-treated rats, there was a significant correlation between 24(S)-HC brain levels and SWDs as measured by EEG (Figure 7b). Chronic AY9944 treatment increased SWDs as measured by the total number and duration of discharges. Post hoc analysis revealed that acute treatment with SAGE-718 significantly reduced AY9944-induced increases in both the total number and duration of SWDs (Figure 7c,d). There was also a significant correlation between 24(S)-HC levels and locomotor activity (Figure 7e). AY9944 treatment also caused a significant increase in both locomotor activity and rearing behaviour, compared with the vehicle group (Figure 7f,g), which is in line with the actions of NMDA receptor open channel blockers on locomotor behaviour (Chartoff et al., 2005). There was a statistically significant effect of SAGE-718 treatment on reducing both AY9944-evoked locomotor activity and rearing behaviour. Post hoc analysis revealed that both 3 and 20 mg·kg^{-1} significantly attenuated AY9944-induced hyperactivity and increased rearing. These data suggest that SAGE-718 attenuates the deficits produced by cholesterol dysregulation and/or reductions in 24(S)-HC levels.

3.5 | SAGE-718 is well tolerated

PAMs of NMDA receptors are promising therapeutic agents for conditions caused by NMDA receptor hypofunction, but excessive glutamatergic transmission can produce deleterious effects such as epileptogenic activity and excitotoxicity. To evaluate the nonclinical safety profile of SAGE-718, we first measured neural activity in rodent cortical cultures with MEA, as these recordings can be used to predict drug-induced epileptiform activity by analysing synchronization (Avoli & Jefferys, 2016). The effect of SAGE-718 on network activity was compared with the effect of vehicle (including up to 0.64% DMSO) to control for drift in activity over the long recording period. Representative raster plots for vehicle and after incubation with SAGE-718 are shown in Figure 8a. SAGE-718 dose-dependently increased spike rate (Figure S8A) and also increased the duration of bursts (Figure S8B). Interestingly, SAGE-718 dose-dependently reduced the number of bursts, as shown by an increase in the IBI (Figure S8C). SAGE-718 did not affect SynAll when compared with a vehicle control (Figure 8b), suggesting that SAGE-718 does not alter synchronicity. These data provide evidence that SAGE-718 enhanced network activity as reflected by increased firing rate and burst duration but did not alter network synchronization, a predictor of epileptiform activity.

To further evaluate epileptogenic potential, SAGE-718 was evaluated in the PTZ-induced seizure model. SAGE-718 (10, 30 and 50 mg·kg^{-1}) did not significantly affect clonic or tonic seizure latency compared with vehicle-treated mice (Table S4; Figure 8c) at the doses measured. In contrast, diazepam, a benzodiazepine and $GABA_A$ receptor PAM, significantly increased latency to both tonic and clonic seizures compared with vehicle-treated mice, while theophylline, an

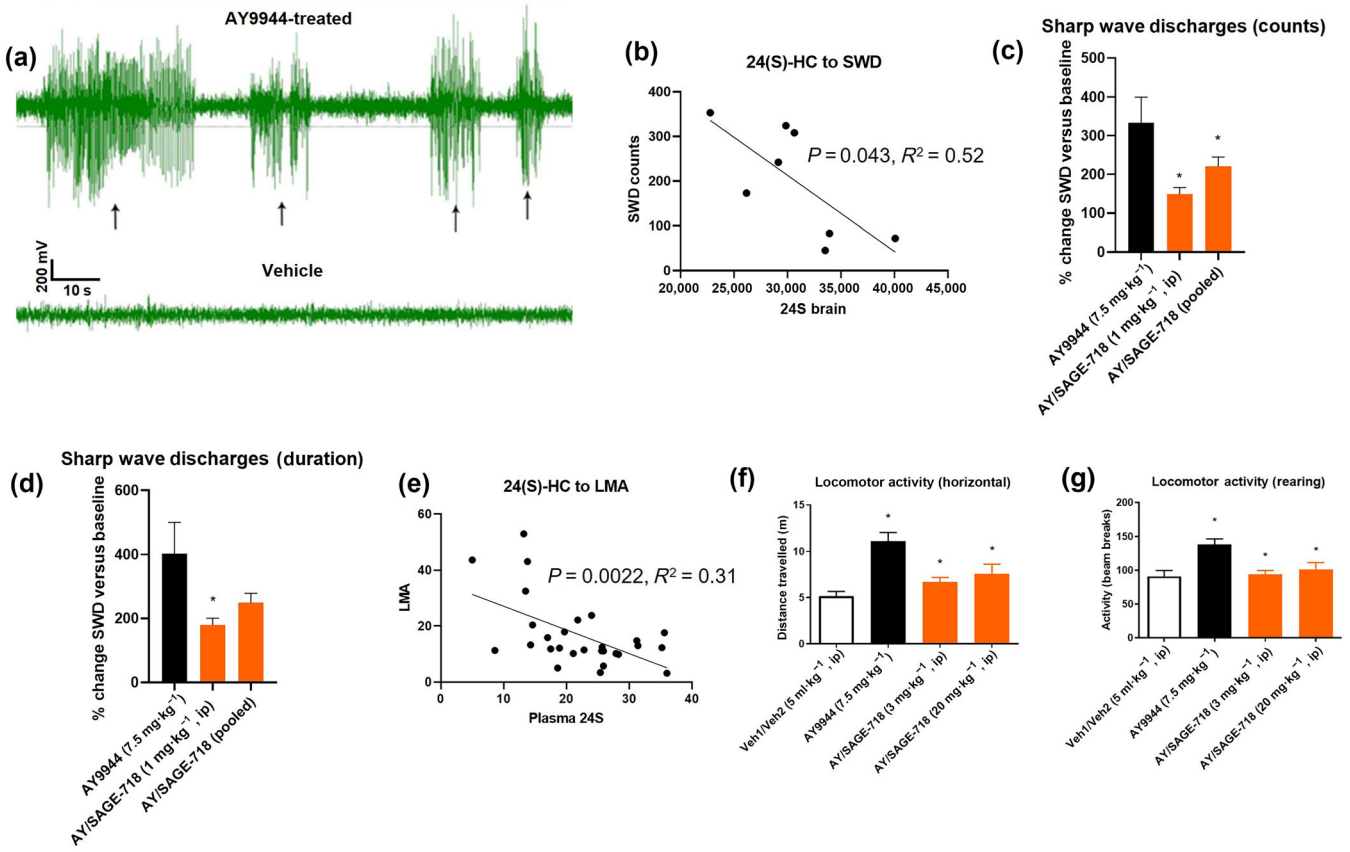

(h)

Dose SAGE-718	Male Plasma C_{max} ($ng \cdot ml^{-1}$ Est.)	Male Plasma AUC ($ng \cdot h^{-1} \cdot ml^{-1}$ Est.)	Male Brain C_{max} ($ng \cdot g^{-1}$ Est.)	Female Plasma C_{max} ($ng \cdot ml^{-1}$ actual)	Female Plasma AUC ($ng \cdot h^{-1} \cdot ml^{-1}$ actual)	Female Brain ($ng \cdot g^{-1}$ actual)
1 $mg \cdot kg^{-1}$, ip	101.5	820.6	103.2	ND	ND	ND
3 $mg \cdot kg^{-1}$, ip	223.3	1805.4	331.8	31.8 ± 1.4	ND	84.7 ± 9.3
10 $mg \cdot kg^{-1}$, ip	281.3	2274	347	ND	ND	ND
20 $mg \cdot kg^{-1}$, ip	ND	ND	ND	68 ± 11.2	ND	98.9 ± 12.3

FIGURE 7 SAGE-718 effects on locomotor activity and sharp wave discharges in the AY9944 model. (a) Representative traces of AY9944-induced sharp wave discharges (SWD). (b) 24(S)-hydroxycholesterol (24(S)-HC) was positively correlated with the number of sharp wave discharges. AY9944 administration increased the number (c) and duration (d) of sharp waves observed on electroencephalogram (EEG) in male rats. SAGE-718 attenuated both the total number and duration of sharp wave discharges at 1 $mg \cdot kg^{-1}$. Pooled group includes both 3 and 10 $mg \cdot kg^{-1}$ cohorts because brain C_{max} values for each dose group were nearly equal. (e) 24(S)-HC was positively correlated with locomotor activity (LMA). AY9944 significantly increased both distance travelled (f) and rearing behaviour (g) in female rats. SAGE-718 attenuated AY9944-induced changes in locomotor activity at 3 and 20 $mg \cdot kg^{-1}$. (h) Exposures measured from test animals in the locomotor activity and EEG experiments. Data shown are means ± SEM from the number of animals as follows: for the SWD assays (in c and d): AY9944, n = 9; SAGE-718 (1mg/kg), n = 10; SAGE-718 (pooled), n = 20. For the assays of locomotor activity (in f and g): Vehicle n = 23; AY9944, n = 12; SAGE-718 (3mg/kg), n = 13; SAGE-718 (20mg/kg), n = 14. *$P < 0.05$ significantly different from AY9944.

adenosine receptor antagonist and proconvulsant (Breidenbach et al., 2020), significantly decreased latency to tonic, but not clonic, seizures compared with vehicle-treated mice. In test mice, SAGE-718 doses of 10, 30 and 50 $mg \cdot kg^{-1}$ reached plasma concentrations of 330 ± 80, 338 ± 204 and 445 ± 324 $ng \cdot ml^{-1}$, respectively (n = 3, mean ± SD), while brain concentrations were 336 ± 102, 303 ± 195 and 304 ± 236 $ng \cdot g^{-1}$, respectively. SAGE-718 had neither pro- nor anti-convulsant effects on PTZ-induced seizures at brain concentrations at least 70-fold higher than the minimally effect brain concentration in the PCP SI model. Furthermore, the lack of effect in the PTZ assay, which is sensitive to neuroactive steroids that are PAMs of $GABA_A$ receptors (Althaus et al., 2020; Hammond et al., 2017), suggests that the primary pharmacological action of SAGE-718 is modulation of NMDA receptors.

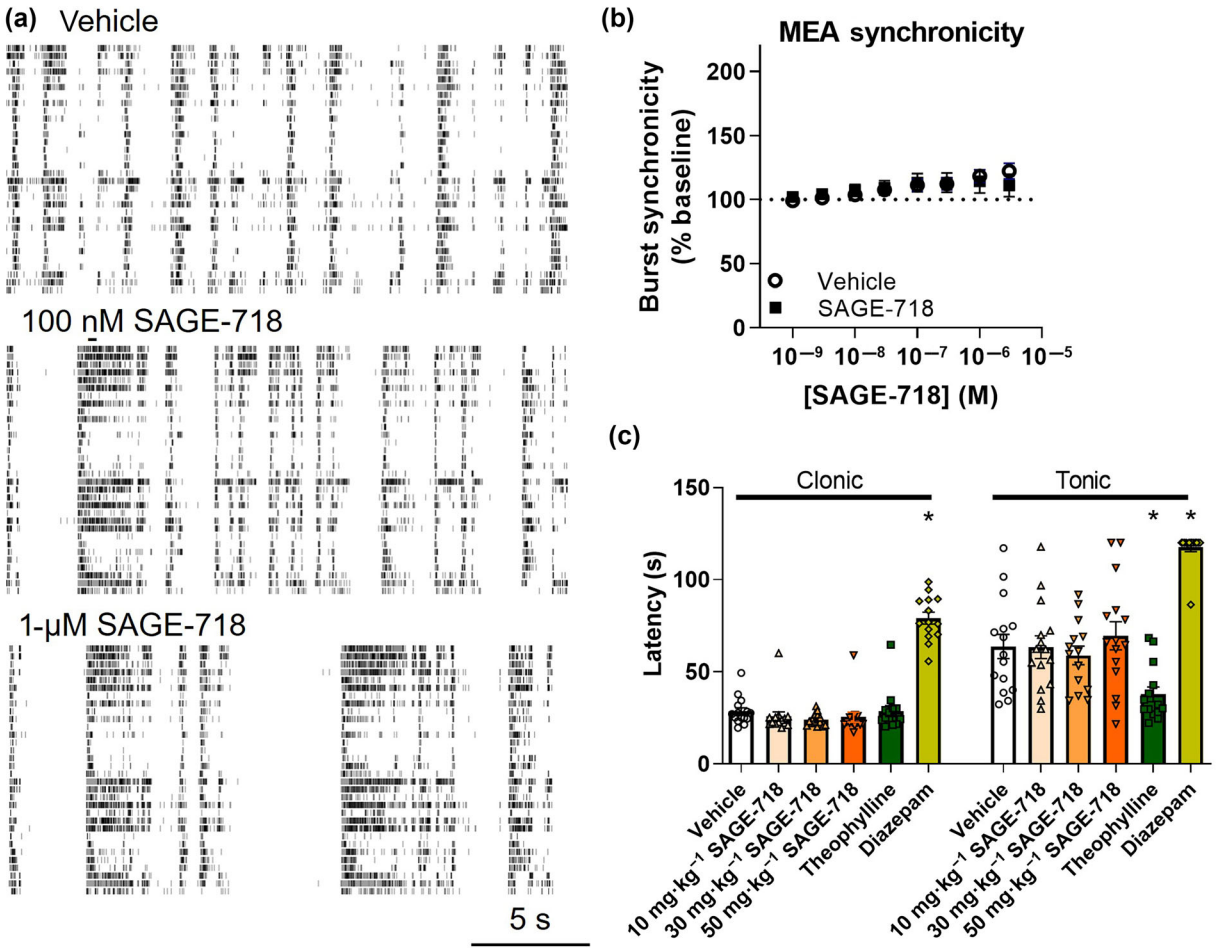

FIGURE 8 SAGE-718 does not produce epileptogenic activity. (a) Representative raster plots of spontaneous activity from cortical cultures with vehicle, 100 nM and 1 μM of SAGE-718. (b) Effects on synchronicity, a measure of the distance of an individual burst away from the population burst centre (n = 8–9 wells per group). (c) Summary of effect of SAGE-718 (i.p., 4 h prior to pentylenetetrazole [PTZ] infusion) on clonic and tonic seizures in mice i.v. infused with PTZ. Diazepam (p.o., 30 min prior to PTZ) and theophylline (i.p., 30 min prior to PTZ) were used as positive controls. Data are shown as mean ± SEM. Doses are expressed as $mg \cdot kg^{-1}$. s = seconds. n = 14–15 animals per group. $^*P < 0.05$, significantly different from vehicle; vehicle versus diazepam: clonic latency, Student's *t* test; tonic latency, Mann–Whitney test; vehicle versus theophylline: tonic latency, Student's *t* test.

Prolonged activation of NMDA receptors can produce excitotoxicity (X. Zhou et al., 2013), so it is critical to evaluate PAMs of these receptors with chronic dosing toxicology testing to rule out potential neurotoxic effects. SAGE-718 was administered once daily oral at dose levels of 0.8, 2.5 and 7 $mg \cdot kg^{-1} \cdot day^{-1}$ to male rats and 2, 6 and 15 $mg \cdot kg^{-1} \cdot day^{-1}$ to female rats for a period of 6 months. Peak plasma concentrations were observed from 2 to 6 h post dose in males and from 0.5 to 2 h post dose in females across all dose levels and evaluation days. Exposure to SAGE-718 increased with overall dose in an approximately dose-proportional manner in males and a less than dose-proportional manner in females on all evaluation days. Accumulation of SAGE-718 in terms of area under the curve at the last time point (AUC_{tlast}) was not observed for males and females, with values that were generally similar on Days 91 and 182 versus Day 1. Administration of SAGE-718 by once daily oral gavage to rats at dose levels of 0.8, 2.5 and 7 $mg \cdot kg^{-1} \cdot day^{-1}$ in males and 2, 6 and 15 $mg \cdot kg^{-1} \cdot day^{-1}$ in females for 182 consecutive days was well tolerated at all doses. There were no SAGE-718-related effects on survival or adverse findings, including no signs of neurodegeneration or neurotoxicity. The no-observed-adverse-effect level (NOAEL) was 7 $mg \cdot kg^{-1} \cdot day^{-1}$ in males and 15 $mg \cdot kg^{-1} \cdot day^{-1}$ in females, which corresponded to mean plasma C_{max} values of 839 and 607 $ng \cdot ml^{-1}$ for males and females, respectively, on Day 182. The estimated brain C_{max} for SAGE-718 at the NOAEL was 1574 $ng \cdot g^{-1}$ for males, which is >300-fold higher than the minimally effective brain concentration in the PCP SI model, clearly demonstrating that SAGE-718 is safe and well tolerated in the target coverage range required for efficacy in a model of NMDA receptor hypofunction (Figure 9).

4 | DISCUSSION

We have characterized the pharmacology of SAGE-718, a novel neuroactive steroid NMDA receptor PAM currently in clinical

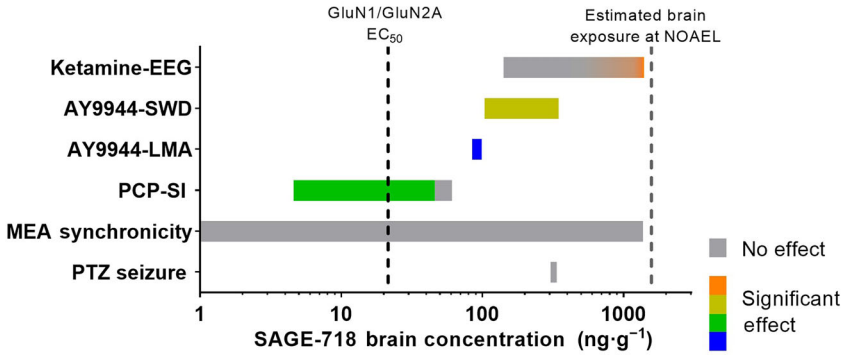

FIGURE 9 Pharmacodynamic profile of SAGE-718. Exposuregram summarizing effects of SAGE-718 on pharmacodynamic and safety studies. No effect—grey; SAGE-718 significantly accelerated return to baseline electroencephalogram (EEG) gamma after ketamine, in rats—orange (solid—significant effect; gradient—pharmacokinetic/pharmacodynamic trend); SAGE-718 reduced sharp wave discharge (SWD) in AY9944-treated rats—yellow; SAGE-718 reduced AY9944-induced hyperactivity—blue; SAGE-718 improved social behaviour in a subchronic phencyclidine (PCP) model in rats—green. Minimally effective brain concentration in the PCP social interaction (SI) model was taken from the high end of the extrapolated concentration range due to drug measurements being below the level of quantification. No effect on MEA synchronicity at any concentration tested or in the pentylenetetrazole (PTZ) seizure model in mice up to a brain exposure of 336 $ng \cdot g^{-1}$. GluN1/GluN2A EC_{50} as measured with manual patch clamp (EC_{50} = 46 nM or 21 $ng \cdot g^{-1}$; Figure 1c). As a reference, $GABA_A$ receptor α1β2γ2 EC_{50} = 570 nM or 260 $ng \cdot g^{-1}$. Estimated brain exposure at rat no-observed-adverse-effect level (NOAEL) was 1574.4 $ng \cdot g^{-1}$ and was calculated by multiplying the plasma C_{max} following 7 $mg \cdot kg^{-1} \cdot day^{-1}$ in male rats (839 $ng \cdot ml^{-1}$) by the calculated C_{max} B:P ratio (B:P = 1.88) in the rat pharmacokinetic study. LMA, locomotor activity.

development for the treatment of cognitive impairment. SAGE-718 increases currents through all di-heteromeric GluN2-containing receptors with near equipotency and produces a leftward shift in the glutamate, glycine and D-serine concentration–response. This mechanism of action, including the <3-fold shift in agonist potency and potentiation of saturating D-serine but not saturating glutamate or glycine, may minimize some of the safety risks associated with positive modulation of NMDA receptors (Hackos & Hanson, 2017). SAGE-718 likely increases channel open probability, which is consistent with faster rates of ketamine block and unblock. Other oxysterol molecules similarly increase the channel open probability of NMDA receptors and rates of channel block and unblock with other NMDA receptor open channel blockers (Emnett et al., 2015; Linsenbardt et al., 2014; Paul et al., 2013). The binding site of SAGE-718 on the channel is likely to overlap with that of 24(S)-HC, with structural determinants including residues in the transmembrane domain of both GluN1 and GluN2 receptor subunits (Tang et al., 2023). SAGE-718 increases NMDA receptor EPSP amplitude in rat striatal medium spiny neurons and network activity in cultured cortical neurons, indicating that activity in recombinant cell lines translates to enhanced synaptic activity and spiking in neurons. Although effects of SAGE-718 on tri-heteromeric receptors were not characterized in this study, the lack of discrimination between GluN2 subunits and potentiation of EPSPs in striatal neurons, which are likely to contain triheteromeric receptors (Dunah et al., 1998; Logan et al., 2007), suggests that these receptors are also sensitive to SAGE-718. Further studies will be needed to understand additional mechanistic details of the mechanism of potentiation.

In line with the in vitro mechanism of action, SAGE-718 accelerates the return to baseline gamma power following administration of ketamine in an EEG study in awake rats. This change in gamma power provides evidence for target engagement in vivo in an NMDA receptor hypofunction state and, beneficially, is a translational endpoint that can be tested clinically (Murck et al., 2019). Prior to ketamine administration, SAGE-718 had no effect on the EEG power spectrum in the wake state. In a previous study profiling an NMDA receptor PAM in EEG, the GluN2A-specific GNE-0723 modulated EEG oscillations across several frequency bands in awake mice (Hanson et al., 2020). The distinct EEG effects of GNE-0273 compared with those of SAGE-718 may relate to structural differences and distinct mechanisms of action and NMDA receptor subtype-selective profiles between the compounds (Geoffroy et al., 2022). While SAGE-718 has modest PAM activity on $GABA_A$ receptors in vitro, at relatively high concentrations (≥1 μM), there was no evidence of a $GABA_A$ receptor-driven EEG signal in the beta frequency band (Figure S5C; Althaus et al., 2020; Mandema & Danhof, 1992), nor were there behavioural signs of sedation, suggesting that $GABA_A$ receptors were not significantly modulated at pharmacologically relevant SAGE-718 doses. Combined with no secondary pharmacology hits on a broad binding target panel or cardiac ion channel panel (Hill et al., 2022), our data provide strong evidence that the behavioural and in vivo electrophysiological effects of SAGE-718 are driven by on-target potentiation of NMDA receptors.

SAGE-718 improved deficits in two preclinical models of NMDA receptor hypofunction: enduring inhibition of NMDA receptors with subchronic PCP administration and reduction of cholesterol and 24(S)-HC with AY9944 administration. Specifically, SAGE-718 increased SI in rats that previously received subchronic PCP, reversing deficits in behaviour produced by sustained NMDA receptor hypofunction, a result comparable to other NMDA receptor PAMs (La et al., 2019; Paul et al., 2013). Subchronic PCP administration is an

established model of schizophrenia, in particular of the negative and cognitive symptoms (G. Lee & Zhou, 2019), and prolonged inhibition of NMDA receptors with PCP produces long-lasting neural maladaptations and concomitant cognitive deficits (Dawson et al., 2014; Jenkins et al., 2008; McKibben et al., 2010). In Huntington's disease, cognitive impairment can include deficits in social cognition, such as recognition of emotions in response to facial and vocal stimuli, which can precede the onset of motor symptoms (Bora et al., 2016; Cavallo et al., 2022; Henley et al., 2012). Furthermore, in individuals with Huntington's disease, 24(S)-HC levels are correlated with several cognitive tasks, including negative emotional processing in the Eckman faces task (Lewis et al., 2020). The impairment in social behaviour produced by persistent NMDA receptor hypofunction may be relevant to a range of neuropsychiatric disorders with observable deficits in social cognition, such as Huntington's disease.

Several disorders, including Huntington's disease and SLOS, are characterized by cholesterol processing deficits (Kreilaus et al., 2016; Leoni et al., 2011). In a model of cholesterol depletion, inhibition of 7-dehydrocholesterol reductase with AY9944 resulted in reduced serum cholesterol levels and decreased plasma and brain 24(S)-HC levels that were negatively correlated with electrophysiological and behavioural changes. Cholesterol depletion reduces hippocampal long-term potentiation (LTP) and deficits in hippocampal-dependent learning (Chan et al., 2004), similar to animals lacking CYP46A1, the enzyme that produces 24(S)-HC (Kotti et al., 2006). These deficits are likely to be linked to NMDA receptor hypofunction, as CYP46A1 knockout mice have greatly reduced 24(S)-HC levels in brain and attenuated synaptic NMDA receptor activity (Sun et al., 2016). Importantly, the alterations produced by AY9944 were reversed with SAGE-718, suggesting that treatment with neuroactive steroid NMDA receptor PAMs may have therapeutic benefit in diseases in which a key pathophysiological feature is dysregulated cholesterol processing.

Alterations in cholesterol and 24(S)-HC levels, NMDA receptor function and cognitive impairment are also evident in Parkinson's and Alzheimer's diseases (Dai et al., 2021; Gamba et al., 2021; Leoni et al., 2013; Papassotiropoulos et al., 2000; Petrov & Pikuleva, 2019). In Huntington's and Parkinson's diseases, mild cognitive symptoms usually occur before the onset of motor disturbances (Marder et al., 2000; Ross & Tabrizi, 2011). Most available therapies will alleviate motor and psychiatric symptoms (Ross & Tabrizi, 2011), and there is an urgent unmet need for therapeutic agents targeting early cognitive impairment. In Huntington's disease, a reduction in 24(S)-HC can be detected in early stages of disease (Leoni et al., 2013), and genetic testing can confirm disease inheritance prior to any symptoms, providing an opportunity for early therapeutic intervention (Kacher et al., 2022). By all measures we have undertaken, SAGE-718 modulates NMDA receptors by a mechanism similar to that of 24(S)-HC (Paul et al., 2013), so SAGE-718 may compensate for the loss of 24(S)-HC modulation of NMDA receptor activity. Further, because of the role that NMDA receptors have been shown to play in neural plasticity, SAGE-718 may improve cognitive impairment and potentially slow cognitive decline associated with neurodegeneration (Geoffroy et al., 2022). In Alzheimer's disease, NMDA receptor antagonists are used to reduce excitotoxicity and neuronal death, which is thought to be due to extrasynaptic GluN2B-containing NMDA receptors (Hardingham et al., 2002; Q. Zhou & Sheng, 2013). These compounds are likely also to block synaptic NMDA receptors, limiting their use for improving cognitive function. Because NMDA receptor PAMs such as SAGE-718 increase receptor activity only in the presence of agonists, they should preferentially activate synaptic receptors and limit excitotoxicity. Consistent with this idea, a GluN2A-specific PAM has been shown to improve cognitive function in preclinical models of Alzheimer's disease (Hanson et al., 2020).

Excessive glutamatergic and NMDA receptor drive can produce epileptogenic activity and excitotoxicity (Hanada, 2020), and some compounds that have PAM activity against other glutamatergic receptors, such as $mGlu_5$, have produced seizures in animal models (Yang et al., 2016). The mechanism of SAGE-718 potentiation should minimize excessive NMDA receptor drive because channel potentiation is diminished when channels are already highly active, as in the presence of maximal agonists or high 24(S)-HC levels. In the MEA assay, while SAGE-718 increased firing rate and burst duration, it had no effect on neural synchronization, an in vitro correlate of epileptiform activity (Avoli & Jefferys, 2016). SAGE-718 did not alter the latency to tonic or clonic seizures in the PTZ infusion assay at brain concentrations up to 336 $ng \cdot g^{-1}$, which is at least 70-fold higher than the minimally effective brain concentration in the PCP SI model. Furthermore, there was no evidence of neurotoxicity in rats administered SAGE-718 once daily for 6 months, and brain exposure at the NOAEL was estimated to be over 300-fold higher than exposures required for efficacy in the PCP SI model. These data provide compelling evidence that SAGE-718 is safe and well tolerated and positively modulates NMDA receptor activity in preclinical models of NMDA receptor hypofunction.

SAGE-718 increases the activity of NMDA receptors via a mechanism similar to that of 24(S)-HC and under conditions of reduced receptor activation, whether due to submaximal agonist concentrations or NMDA receptor hypofunction. Positive modulation of NMDA receptor activity rescued SI deficits due to NMDA receptor hypofunction and changes in EEG activity due to acute NMDA receptor block. Given the role of NMDA receptors in neuronal plasticity and memory formation, SAGE-718 may improve cognitive impairment in patients with neurodegenerative diseases and other behavioural deficits due to NMDA receptor hypofunction and potentially afford a novel treatment for a number of debilitating diseases. Currently, SAGE-718 has received Fast Track Designation by Food and Drug Administration (FDA) and Orphan Drug Designation by the European Medicines Agency for treatment of cognitive deficits in Huntington's disease and is being investigated clinically (NCT05107128). Modulation of NMDA receptors with SAGE-718 may therefore be a promising new therapy for treating cognitive impairment associated with a variety of neurodegenerative diseases.

AUTHOR CONTRIBUTIONS

J. T. Beckley: Conceptualization (supporting); formal analysis (equal); methodology (equal); project administration (equal); visualization (lead); writing—original draft (lead); writing—review and editing (equal).

T. K. Aman: Conceptualization (supporting); data curation (supporting); methodology (equal); project administration (equal); visualization (equal); writing—original draft (lead); writing—review and editing (equal). **M. A. Ackley:** Conceptualization (equal); data curation (equal); investigation (equal); project administration (equal); supervision; writing—review and editing (supporting). **T. M. Kazdoba:** Data curation (equal); formal analysis (equal); methodology (equal); project administration (equal); writing—original draft (supporting); writing—review and editing (equal). **M. C. Lewis:** Conceptualization (supporting); formal analysis (equal); methodology (equal); project administration (equal); visualization (supporting); writing—original draft (supporting); writing—review and editing (equal). **A. C. Smith:** Conceptualization (supporting); formal analysis (lead); methodology (equal); visualization (equal); writing—original draft (supporting); writing—review and editing (equal). **B. J. Farley:** Conceptualization (equal); formal analysis (supporting); methodology (equal); visualization (supporting); writing—review and editing (equal). **J. Dai:** Formal analysis (equal); methodology (equal); project administration (equal); writing—original draft (supporting); writing—review and editing (equal). **W. Deats:** Conceptualization (equal); methodology (equal); project administration (equal); writing—original draft (supporting); writing—review and editing (equal). **E. Hoffmann:** Conceptualization (equal); investigation (equal); project administration (equal); supervision (equal); writing—review and editing (equal). **A. J. Robichaud:** Investigation (equal); methodology (equal); supervision (equal); writing—review and editing (equal). **J. J. Doherty:** Conceptualization (equal); project administration (equal); supervision (lead); writing—review and editing (equal). **M. C. Quirk:** Conceptualization (equal); investigation (equal); project administration (equal); supervision (lead); writing—original draft (supporting); writing—review and editing (equal).

ACKNOWLEDGEMENTS

We would like to acknowledge and thank Francesco G. Salituro, Gabriel Martinez Botella and Gabriel M. Belfort for their work that led to the discovery of SAGE-718. We would also like to thank Negah Rahmati, Carolyn Johnson, Carla Maciag and Rebecca Hammond for their contributions to this manuscript. All studies were funded by Sage Therapeutics.

CONFLICT OF INTEREST STATEMENT

All authors are employees and shareholders of Sage Therapeutics.

DATA AVAILABILITY STATEMENT

The data that support the findings of this study are available from the corresponding author upon reasonable request. Some data may not be made available because of privacy or ethical restrictions.

DECLARATION OF TRANSPARENCY AND SCIENTIFIC RIGOUR

This Declaration acknowledges that this paper adheres to the principles for transparent reporting and scientific rigour of preclinical research as stated in the *BJP* guidelines for Design and Analysis, and Animal Experimentation, and as recommended by funding agencies, publishers and other organizations engaged with supporting research.

ORCID

Jacob T. Beckley https://orcid.org/0000-0003-2950-6462

REFERENCES

Akk, G., Bracamontes, J., & Steinbach, J. H. (2001). Pregnenolone sulfate block of GABAA receptors: Mechanism and involvement of a residue in the M2 region of the α subunit. *The Journal of Physiology*, *532*(3), 673–684. https://doi.org/10.1111/j.1469-7793.2001.0673e.x

Alexander, S. P., Christopoulos, A., Davenport, A. P., Kelly, E., Mathie, A., Peters, J. A., Veale, E. L., Armstrong, J. F., Faccenda, E., Harding, S. D., Pawson, A. J., Southan, C., Davies, J. A., Abbracchio, M. P., Alexander, W., Al-hosaini, K., Bäck, M., Barnes, N. M., Bathgate, R., … Ye, R. D. (2021). THE CONCISE GUIDE TO PHARMACOLOGY 2021/22: G protein-coupled receptors. *British Journal of Pharmacology*, *178*(S1), S27–S156. https://doi.org/10.1111/bph.15538

Alexander, S. P., Fabbro, D., Kelly, E., Mathie, A., Peters, J. A., Veale, E. L., Armstrong, J. F., Faccenda, E., Harding, S. D., Pawson, A. J., Southan, C., Davies, J. A., Boison, D., Burns, K. E., Dessauer, C., Gertsch, J., Helsby, N. A., Izzo, A. A., Koesling, D., … Wong, S. S. (2021). THE CONCISE GUIDE TO PHARMACOLOGY 2021/22: Enzymes. *British Journal of Pharmacology*, *178*(S1), S313–S411. https://doi.org/10.1111/bph.15542

Alexander, S. P., Mathie, A., Peters, J. A., Veale, E. L., Striessnig, J., Kelly, E., Armstrong, J. F., Faccenda, E., Harding, S. D., Pawson, A. J., Southan, C., Davies, J. A., Aldrich, R. W., Attali, B., Baggetta, A. M., Becirovic, E., Biel, M., Bill, R. M., Catterall, W. A., … Zhu, M. (2021). THE CONCISE GUIDE TO PHARMACOLOGY 2021/22: Ion channels. *British Journal of Pharmacology*, *178*(S1), S157–S245. https://doi.org/10.1111/bph.15539

Althaus, A. L., Ackley, M. A., Belfort, G. M., Gee, S. M., Dai, J., Nguyen, D. P., Kazdoba, T. M., Modgil, A., Davies, P. A., Moss, S. J., Salituro, F. G., Hoffmann, E., Hammond, R. S., Robichaud, A. J., Quirk, M. C., & Doherty, J. J. (2020). Preclinical characterization of zuranolone (SAGE-217), a selective neuroactive steroid GABAA receptor positive allosteric modulator. *Neuropharmacology*, *181*, 108333. https://doi.org/10.1016/j.neuropharm.2020.108333

Anticevic, A., Gancsos, M., Murray, J. D., Repovs, G., Driesen, N. R., Ennis, D. J., Niciu, M. J., Morgan, P. T., Surti, T. S., Bloch, M. H., Ramani, R., Smith, M. A., Wang, X. J., Krystal, J. H., & Corlett, P. R. (2012). NMDA receptor function in large-scale anticorrelated neural systems with implications for cognition and schizophrenia. *Proceedings of the National Academy of Sciences*, *109*(41), 16720–16725. https://doi.org/10.1073/pnas.1208494109

Avoli, M., & Jefferys, J. G. (2016). Models of drug-induced epileptiform synchronization in vitro. *Journal of Neuroscience Methods*, *260*, 26–32. https://doi.org/10.1016/j.jneumeth.2015.10.006

Björkhem, I., Starck, L., Andersson, U., Lütjohann, D., von Bahr, S., Pikuleva, I., Babiker, A., & Diczfalusy, U. (2001). Oxysterols in the circulation of patients with the Smith-Lemli-Opitz syndrome: Abnormal levels of 24S- and 27-hydroxycholesterol. *Journal of Lipid Research*, *42*(3), 366–371. https://doi.org/10.1016/S0022-2275(20)31660-6

Bora, E., Velakoulis, D., & Walterfang, M. (2016). Social cognition in Huntington's disease: A meta-analysis. *Behavioural Brain Research*, *297*, 131–140. https://doi.org/10.1016/j.bbr.2015.10.001

Breidenbach, L., Hempel, K., Mittelstadt, S. W., & Lynch, J. J. 3rd. (2020). Refinement of the rodent pentylenetetrazole proconvulsion assay, which is a good predictor of convulsions in repeat-dose toxicology studies. *Journal of Pharmacological and Toxicological Methods*, *101*, 106653. https://doi.org/10.1016/j.vascn.2019.106653

Cavallo, M., Sergi, A., & Pagani, M. (2022). Cognitive and social cognition deficits in Huntington's disease differ between the prodromal and the manifest stages of the condition: A scoping review of recent evidence. *The British Journal of Clinical Psychology*, *61*(2), 214–241. https://doi.org/10.1111/bjc.12337

Chan, K. F., Jia, Z., Murphy, P. A., Burnham, W. M., Cortez, M. A., & Snead, O. C. 3rd. (2004). Learning and memory impairment in rats with chronic atypical absence seizures. *Experimental Neurology*, *190*(2), 328–336. https://doi.org/10.1016/j.expneurol.2004.08.001

Chartoff, E. H., Heusner, C. L., & Palmiter, R. D. (2005). Dopamine is not required for the hyperlocomotor response to NMDA receptor antagonists. *Neuropsychopharmacology*, *30*(7), 1324–1333. https://doi.org/10.1038/sj.npp.1300678

Curtis, M. J., Alexander, S. P. H., Cirino, G., George, C. H., Kendall, D. A., Insel, P. A., Izzo, A. A., Ji, Y., Panettieri, R. A., Patel, H. H., Sobey, C. G., Stanford, S. C., Stanley, P., Stefanska, B., Stephens, G. J., Teixeira, M. M., Vergnolle, N., & Ahluwalia, A. (2022). Planning experiments: Updated guidance on experimental design and analysis and their reporting III. *British Journal of Pharmacology*, *179*, 3907–3913. https://doi.org/10.1111/bph.15868

Dai, L., Zou, L., Meng, L., Qiang, G., Yan, M., & Zhang, Z. (2021). Cholesterol metabolism in neurodegenerative diseases: Molecular mechanisms and therapeutic targets. *Molecular Neurobiology*, *58*(5), 2183–2201. https://doi.org/10.1007/s12035-020-02232-6

Dawson, N., Xiao, X., McDonald, M., Higham, D. J., Morris, B. J., & Pratt, J. A. (2014). Sustained NMDA receptor hypofunction induces compromised neural systems integration and schizophrenia-like alterations in functional brain networks. *Cerebral Cortex*, *24*(2), 452–464. https://doi.org/10.1093/cercor/bhs322

Dunah, A. W., Luo, J., Wang, Y. H., Yasuda, R. P., & Wolfe, B. B. (1998). Subunit composition of N-methyl-D-aspartate receptors in the central nervous system that contain the NR2D subunit. *Molecular Pharmacology*, *53*(3), 429–437. https://doi.org/10.1124/mol.53.3.429

Emnett, C. M., Eisenman, L. N., Mohan, J., Taylor, A. A., Doherty, J. J., Paul, S. M., Zorumski, C. F., & Mennerick, S. (2015). Interaction between positive allosteric modulators and trapping blockers of the NMDA receptor channel. *British Journal of Pharmacology*, *172*(5), 1333–1347. https://doi.org/10.1111/bph.13007

Fernandes, H. B., & Raymond, L. A. (2009). NMDA receptors and Huntington's disease. In A.M. Van Dongen (Ed.), *Biology of the NMDA receptor* (pp. 17–40). CRC Press/Taylor & Francis.

Gamba, P., Giannelli, S., Staurenghi, E., Testa, G., Sottero, B., Biasi, F., Poli, G., & Leonarduzzi, G. (2021). The controversial role of 24-S-hydroxycholesterol in Alzheimer's disease. *Antioxidants (Basel)*, *10*(5), 740. https://doi.org/10.3390/antiox10050740

Geoffroy, C., Paoletti, P., & Mony, L. (2022). Positive allosteric modulation of NMDA receptors: Mechanisms, physiological impact and therapeutic potential. *The Journal of Physiology*, *600*(2), 233–259. https://doi.org/10.1113/JP280875

Gramowski-Voß, A., Schwertle, H.-J., Pielka, A.-M., Schultz, L., Steder, A., Jügelt, K., Axmann, J., & Pries, W. (2015). Enhancement of cortical network activity in vitro and promotion of GABAergic neurogenesis by stimulation with an electromagnetic field with a 150 MHz carrier wave pulsed with an alternating 10 and 16 Hz modulation. *Frontiers in Neurology*, *6*, 158. https://doi.org/10.3389/fneur.2015.00158

Grayson, B., Idris, N., & Neill, J. (2007). Atypical antipsychotics attenuate a sub-chronic PCP-induced cognitive deficit in the novel object recognition task in the rat. *Behavioural Brain Research*, *184*(1), 31–38. https://doi.org/10.1016/j.bbr.2007.06.012

Hackos, D. H., & Hanson, J. E. (2017). Diverse modes of NMDA receptor positive allosteric modulation: Mechanisms and consequences. *Neuropharmacology*, *112*(Pt A), 34–45. https://doi.org/10.1016/j.neuropharm.2016.07.037

Hammond, R. S., Althaus, A. L., Ackley, M. A., Maciag, C., Martinez Botella, G., Salituro, F. G., Robichaud, A. J., & Doherty, J. J. (2017). Anticonvulsant profile of the neuroactive steroid, SGE-516, in animal models. *Epilepsy Research*, *134*, 16–25. https://doi.org/10.1016/j.eplepsyres.2017.05.001

Hanada, T. (2020). Ionotropic glutamate receptors in epilepsy: A review focusing on AMPA and NMDA receptors. *Biomolecules*, *10*(3), 464. https://doi.org/10.3390/biom10030464

Hanson, J. E., Ma, K., Elstrott, J., Weber, M., Saillet, S., Khan, A. S., Simms, J., Liu, B., Kim, T. A., Yu, G. Q., Chen, Y., Wang, T. M., Jiang, Z., Liederer, B. M., Deshmukh, G., Solanoy, H., Chan, C., Sellers, B. D., Volgraf, M., … Palop, J. J. (2020). GluN2A NMDA receptor enhancement improves brain oscillations, synchrony, and cognitive functions in Dravet syndrome and Alzheimer's disease models. *Cell Reports*, *30*(2), 381–396.e384. https://doi.org/10.1016/j.celrep.2019.12.030

Hardingham, G. E., Fukunaga, Y., & Bading, H. (2002). Extrasynaptic NMDARs oppose synaptic NMDARs by triggering CREB shut-off and cell death pathways. *Nature Neuroscience*, *5*(5), 405–414. https://doi.org/10.1038/nn835

Hedegaard, M., Hansen, K. B., Andersen, K. T., Bräuner-Osborne, H., & Traynelis, S. F. (2012). Molecular pharmacology of human NMDA receptors. *Neurochemistry International*, *61*(4), 601–609. https://doi.org/10.1016/j.neuint.2011.11.016

Henley, S. M., Novak, M. J., Frost, C., King, J., Tabrizi, S. J., & Warren, J. D. (2012). Emotion recognition in Huntington's disease: A systematic review. *Neuroscience and Biobehavioral Reviews*, *36*(1), 237–253. https://doi.org/10.1016/j.neubiorev.2011.06.002

Hill, M. D., Blanco, M. J., Salituro, F. G., Bai, Z., Beckley, J. T., Ackley, M. A., Dai, J., Doherty, J. J., Harrison, B. L., Hoffmann, E. C., Kazdoba, T. M., Lanzetta, D., Lewis, M., Quirk, M. C., & Robichaud, A. J. (2022). SAGE-718: A first-in-class N-methyl-D-aspartate receptor positive allosteric modulator for the potential treatment of cognitive impairment. *Journal of Medicinal Chemistry*, *65*(13), 9063–9075. https://doi.org/10.1021/acs.jmedchem.2c00313

Hogg, R. C., Bandelier, F., Benoit, A., Dosch, R., & Bertrand, D. (2008). An automated system for intracellular and intranuclear injection. *Journal of Neuroscience Methods*, *169*(1), 65–75. https://doi.org/10.1016/j.jneumeth.2007.11.028

Ishikawa, M., Yoshitomi, T., Covey, D. F., Zorumski, C. F., & Izumi, Y. (2018). Neurosteroids and oxysterols as potential therapeutic agents for glaucoma and Alzheimer's disease. *Neuropsychiatry*, *8*(1), 344–359. https://doi.org/10.4172/Neuropsychiatry.1000356

Jenkins, T. A., Harte, M. K., McKibben, C. E., Elliott, J. J., & Reynolds, G. P. (2008). Disturbances in social interaction occur along with pathophysiological deficits following sub-chronic phencyclidine administration in the rat. *Behavioural Brain Research*, *194*(2), 230–235. https://doi.org/10.1016/j.bbr.2008.07.020

Kacher, R., Mounier, C., Caboche, J., & Betuing, S. (2022). Altered cholesterol homeostasis in Huntington's disease. *Frontiers in Aging Neuroscience*, *14*, 797220. https://doi.org/10.3389/fnagi.2022.797220

Kocsis, B. (2012). Differential role of NR2A and NR2B subunits in N-methyl-D-aspartate receptor antagonist-induced aberrant cortical gamma oscillations. *Biological Psychiatry*, *71*(11), 987–995. https://doi.org/10.1016/j.biopsych.2011.10.002

Kotti, T. J., Ramirez, D. M., Pfeiffer, B. E., Huber, K. M., & Russell, D. W. (2006). Brain cholesterol turnover required for geranylgeraniol production and learning in mice. *Proceedings of the National Academy of Sciences of the United States of America*, *103*(10), 3869–3874. https://doi.org/10.1073/pnas.0600316103

Kreilaus, F., Spiro, A. S., McLean, C. A., Garner, B., & Jenner, A. M. (2016). Evidence for altered cholesterol metabolism in Huntington's disease post mortem brain tissue. *Neuropathology and Applied Neurobiology*, *42*(6), 535–546. https://doi.org/10.1111/nan.12286

La, D. S., Salituro, F. G., Martinez Botella, G., Griffin, A. M., Bai, Z., Ackley, M. A., Dai, J., Doherty, J. J., Harrison, B. L., Hoffmann, E. C., Kazdoba, T. M., Lewis, M. C., Quirk, M. C., & Robichaud, A. J. (2019).

Neuroactive steroid N-methyl-D-aspartate receptor positive allosteric modulators: Synthesis, SAR, and pharmacological activity. *Journal of Medicinal Chemistry*, *62*(16), 7526–7542. https://doi.org/10.1021/acs.jmedchem.9b00591

Lee, B., Pothula, S., Wu, M., Kang, H., Girgenti, M. J., Picciotto, M. R., DiLeone, R. J., Taylor, J. R., & Duman, R. S. (2022). Positive modulation of N-methyl-D-aspartate receptors in the mPFC reduces the spontaneous recovery of fear. *Molecular Psychiatry*, *27*, 2580–2589. https://doi.org/10.1038/s41380-022-01498-7

Lee, G., & Zhou, Y. (2019). NMDAR hypofunction animal models of schizophrenia. *Frontiers in Molecular Neuroscience*, *12*, 185. https://doi.org/10.3389/fnmol.2019.00185

Leoni, V., Long, J. D., Mills, J. A., Di Donato, S., Paulsen, J. S., & group, P.-H. s. (2013). Plasma 24S-hydroxycholesterol correlation with markers of Huntington disease progression. *Neurobiology of Disease*, *55*, 37–43. https://doi.org/10.1016/j.nbd.2013.03.013

Leoni, V., Mariotti, C., Nanetti, L., Salvatore, E., Squitieri, F., Bentivoglio, A. R., Bandettini del Poggio, M., Piacentini, S., Monza, D., Valenza, M., Cattaneo, E., & di Donato, S. (2011). Whole body cholesterol metabolism is impaired in Huntington's disease. *Neuroscience Letters*, *494*(3), 245–249. https://doi.org/10.1016/j.neulet.2011.03.025

Leoni, V., Mariotti, C., Tabrizi, S. J., Valenza, M., Wild, E. J., Henley, S. M., Hobbs, N. Z., Mandelli, M. L., Grisoli, M., Björkhem, I., Cattaneo, E., & di Donato, S. (2008). Plasma 24S-hydroxycholesterol and caudate MRI in pre-manifest and early Huntington's disease. *Brain*, *131*(11), 2851–2859. https://doi.org/10.1093/brain/awn212

Leoni, V., Masterman, T., Diczfalusy, U., De Luca, G., Hillert, J., & Bjorkhem, I. (2002). Changes in human plasma levels of the brain specific oxysterol 24S-hydroxycholesterol during progression of multiple sclerosis. *Neuroscience Letters*, *331*(3), 163–166. https://doi.org/10.1016/S0304-3940(02)00887-X

Lewis, M., Dai, J., Mohan, A., Tabrizi, S., Doherty, J., Robichaud, A., & Quirk, M. (2020). 24(S)-hydroxycholesterol levels are decreased in early Huntington's disease and are associated with deficits in several cognitive domains (4070). *Neurology*, *94*(15 Supplement), 4070.

Lilley, E., Stanford, S. C., Kendall, D. E., Alexander, S. P., Cirino, G., Docherty, J. R., George, C. H., Insel, P. A., Izzo, A. A., Ji, Y., Panettieri, R. A., Sobey, C. G., Stefanska, B., Stephens, G., Teixeira, M., & Ahluwalia, A. (2020). ARRIVE 2.0 and the *British Journal of Pharmacology*: Updated guidance for 2020. *British Journal of Pharmacology*, *177*(16), 3611–3616. https://doi.org/10.1111/bph.15178

Linsenbardt, A. J., Taylor, A., Emnett, C. M., Doherty, J. J., Krishnan, K., Covey, D. F., Paul, S. M., Zorumski, C. F., & Mennerick, S. (2014). Different oxysterols have opposing actions at N-methyl-D-aspartate receptors. *Neuropharmacology*, *85*, 232–242. https://doi.org/10.1016/j.neuropharm.2014.05.027

Logan, S. M., Partridge, J. G., Matta, J. A., Buonanno, A., & Vicini, S. (2007). Long-lasting NMDA receptor-mediated EPSCs in mouse striatal medium spiny neurons. *Journal of Neurophysiology*, *98*(5), 2693–2704. https://doi.org/10.1152/jn.00462.2007

Lü, W., Du, J., Goehring, A., & Gouaux, E. (2017). Cryo-EM structures of the triheteromeric NMDA receptor and its allosteric modulation. *Science*, *355*(6331), eaal3729. https://doi.org/10.1126/science.aal3729

Mandema, J. W., & Danhof, M. (1992). Electroencephalogram effect measures and relationships between pharmacokinetics and pharmacodynamics of centrally acting drugs. *Clinical Pharmacokinetics*, *23*(3), 191–215. https://doi.org/10.2165/00003088-199223030-00003

Marder, K., Zhao, H., Myers, R. H., Cudkowicz, M., Kayson, E., Kieburtz, K., Orme, C., Paulsen, J., Penney, J. B., Siemers, E., & Shoulson, I. (2000). Rate of functional decline in Huntington's disease. *Neurology*, *54*(2), 452. https://doi.org/10.1212/WNL.54.2.452

McKibben, C. E., Jenkins, T. A., Adams, H. N., Harte, M. K., & Reynolds, G. P. (2010). Effect of pretreatment with risperidone on phencyclidine-induced disruptions in object recognition memory and prefrontal cortex parvalbumin immunoreactivity in the rat. *Behavioural Brain Research*, *208*(1), 132–136. https://doi.org/10.1016/j.bbr.2009.11.018

Murck, H., Koenig, A., Berlin, J., Luo, Y., Li, S., Farley, B., Nguyen, D., Webster, I., Quirk, M., Kanes, S., & Doherty, J. (2019). ACNP 58(th) annual meeting: Poster session I. M144: Using a multimodal biomarker approach to identify functional target engagement of the novel NMDA positive allosteric modulator SAGE-718. *Neuropsychopharmacology*, *44*(Suppl 1), 78–229.

Nicoll, R. A., & Roche, K. W. (2013). Long-term potentiation: Peeling the onion. *Neuropharmacology*, *74*, 18–22. https://doi.org/10.1016/j.neuropharm.2013.02.010

Nowaczyk, M. J., & Irons, M. B. (2012). Smith-Lemli-Opitz syndrome: Phenotype, natural history, and epidemiology. *American Journal of Medical Genetics. Part C, Seminars in Medical Genetics*, *160c*(4), 250–262. https://doi.org/10.1002/ajmg.c.31343

Orser, B. A., Pennefather, P. S., & MacDonald, J. F. (1997). Multiple mechanisms of ketamine blockade of N-methyl-D-aspartate receptors. *Anesthesiology*, *86*(4), 903–917. https://doi.org/10.1097/00000542-199704000-00021

Papassotiropoulos, A., Lütjohann, D., Bagli, M., Locatelli, S., Jessen, F., Rao, M. L., Maier, W., Björkhem, I., von Bergmann, K., & Heun, R. (2000). Plasma 24S-hydroxycholesterol: A peripheral indicator of neuronal degeneration and potential state marker for Alzheimer's disease. *Neuroreport*, *11*(9), 1959–1962. https://doi.org/10.1097/00001756-200006260-00030

Paul, S. M., Doherty, J. J., Robichaud, A. J., Belfort, G. M., Chow, B. Y., Hammond, R. S., Crawford, D. C., Linsenbardt, A. J., Shu, H. J., Izumi, Y., Mennerick, S. J., & Zorumski, C. F. (2013). The major brain cholesterol metabolite 24(S)-hydroxycholesterol is a potent allosteric modulator of N-methyl-D-aspartate receptors. *Journal of Neuroscience*, *33*(44), 17290–17300. https://doi.org/10.1523/JNEUROSCI.2619-13.2013

Percie du Sert, N., Hurst, V., Ahluwalia, A., Alam, S., Avey, M. T., Baker, M., Browne, W. J., Clark, A., Cuthill, I. C., Dirnagl, U., Emerson, M., Garner, P., Holgate, S. T., Howells, D. W., Karp, N. A., Lazic, S. E., Lidster, K., MacCallum, C. J., Macleod, M., … Würbel, H. (2020). The ARRIVE guidelines 2.0: Updated guidelines for reporting animal research. *PLoS Biology*, *18*(7), e3000410. https://doi.org/10.1371/journal.pbio.3000410

Petrov, A. M., & Pikuleva, I. A. (2019). Cholesterol 24-hydroxylation by CYP46A1: Benefits of modulation for brain diseases. *Neurotherapeutics*, *16*(3), 635–648. https://doi.org/10.1007/s13311-019-00731-6

Popiolek, M., Izumi, Y., Hopper, A. T., Dai, J., Miller, S., Shu, H.-J., Zorumski, C. F., & Mennerick, S. (2020). Effects of CYP46A1 inhibition on long-term-depression in hippocampal slices ex vivo and 24S-hydroxycholesterol levels in mice in vivo. *Frontiers in Molecular Neuroscience*, *13*, 568641. https://doi.org/10.3389/fnmol.2020.568641

Prerau, M. J., Brown, R. E., Bianchi, M. T., Ellenbogen, J. M., & Purdon, P. L. (2017). Sleep neurophysiological dynamics through the lens of multitaper spectral analysis. *Physiology*, *32*(1), 60–92. https://doi.org/10.1152/physiol.00062.2015

Ross, C. A., & Tabrizi, S. J. (2011). Huntington's disease: From molecular pathogenesis to clinical treatment. *The Lancet Neurology*, *10*(1), 83–98. https://doi.org/10.1016/S1474-4422(10)70245-3

Snigdha, S., & Neill, J. C. (2008). Efficacy of antipsychotics to reverse phencyclidine-induced social interaction deficits in female rats—A preliminary investigation. *Behavioural Brain Research*, *187*(2), 489–494. https://doi.org/10.1016/j.bbr.2007.10.012

Sun, M. Y., Izumi, Y., Benz, A., Zorumski, C. F., & Mennerick, S. (2016). Endogenous 24S-hydroxycholesterol modulates NMDAR-mediated function in hippocampal slices. *Journal of Neurophysiology*, *115*(3), 1263–1272. https://doi.org/10.1152/jn.00890.2015

Tang, W., Beckley, J. T., Zhang, J., Song, R., Xu, Y., Kim, S., Quirk, M. C., Robichaud, A. J., Diaz, E. S., Myers, S. J., Doherty, J. J., Ackley, M. A.,

Traynelis, S. F., & Yuan, H. (2023). Novel neuroactive steroids as positive allosteric modulators of NMDA receptors: Mechanism, site of action, and rescue pharmacology on GRIN variants associated with neurological conditions. *Cellular and Molecular Life Sciences*, *80*(2), 42. https://doi.org/10.1007/s00018-022-04667-7

Traynelis, S. F., Wollmuth, L. P., McBain, C. J., Menniti, F. S., Vance, K. M., Ogden, K. K., Hansen, K. B., Yuan, H., Myers, S. J., & Dingledine, R. (2010). Glutamate receptor ion channels: Structure, regulation, and function. *Pharmacological Reviews*, *62*(3), 405–496. https://doi.org/10.1124/pr.109.002451

Vance, J. E. (2012). Dysregulation of cholesterol balance in the brain: Contribution to neurodegenerative diseases. *Disease Models & Mechanisms*, *5*(6), 746–755. https://doi.org/10.1242/dmm.010124

Wu, F. S., Gibbs, T. T., & Farb, D. H. (1991). Pregnenolone sulfate: A positive allosteric modulator at the N-methyl-D-aspartate receptor. *Molecular Pharmacology*, *40*(3), 333–336.

Yang, F., Snyder, L. B., Balakrishnan, A., Brown, J. M., Sivarao, D. V., Easton, A., Fernandes, A., Gulianello, M., Hanumegowda, U. M., Huang, H., Huang, Y., Jones, K. M., Li, Y. W., Matchett, M., Mattson, G., Miller, R., Santone, K. S., Senapati, A., Shields, E. E., … Degnan, A. P. (2016). Discovery and preclinical evaluation of BMS-955829, a potent positive allosteric modulator of mGluR5. *ACS Medicinal Chemistry Letters*, *7*(3), 289–293. https://doi.org/10.1021/acsmedchemlett.5b00450

Zhang, D.-H., Zhou, X.-D., & Zhou, W.-S. (2002). A short and highly stereoselective synthesis of cerebrosterol. *Chinese Journal of Chemistry*, *20*(11), 1145–1148. https://doi.org/10.1002/cjoc.20020201104

Zhou, Q., & Sheng, M. (2013). NMDA receptors in nervous system diseases. *Neuropharmacology*, *74*, 69–75. https://doi.org/10.1016/j.neuropharm.2013.03.030

Zhou, X., Hollern, D., Liao, J., Andrechek, E., & Wang, H. (2013). NMDA receptor-mediated excitotoxicity depends on the coactivation of synaptic and extrasynaptic receptors. *Cell Death & Disease*, *4*(3), e560. https://doi.org/10.1038/cddis.2013.82

SUPPORTING INFORMATION

Additional supporting information can be found online in the Supporting Information section at the end of this article.

How to cite this article: Beckley, J. T., Aman, T. K., Ackley, M. A., Kazdoba, T. M., Lewis, M. C., Smith, A. C., Farley, B. J., Dai, J., Deats, W., Hoffmann, E., Robichaud, A. J., Doherty, J. J., & Quirk, M. C. (2024). Pharmacological characterization of SAGE-718, a novel positive allosteric modulator of N-methyl-D-aspartate receptors. *British Journal of Pharmacology*, *181*(7), 1028–1050. https://doi.org/10.1111/bph.16235